Pergamon

Bioorganic & Medicinal Chemistry 10 (2002) 1967–1972

BIOORGANIC & MEDICINAL CHEMISTRY

Chemical Modification of the β-Glucocerebrosidase Inhibitor *N*-Octyl-β-valienamine: Synthesis and Biological Evaluation of 4-Epimeric and 4-*O*-(β-D-Galactopyranosyl) Derivatives

Seiichiro Ogawa,[a,*] Yuko Kobayashi Matsunaga[a] and Yoshiyuki Suzuki[b]

[a]*Department of Applied Chemistry, Faculty of Science and Technology, Keio University, Hiyoshi, Kohoku-ku, Yokohama, 223–8522 Japan*
[b]*Nasu Institute for Developmental Disabilities, International University of Health and Welfare, 2600-7 Kita-Kanemaru, Otawara, 324-0011 Japan*

Received 9 October 2001; accepted 14 December 2001

Abstract—*N*-Octyl-β-valienemine (**1**), a potent β-glucocerebrosidase inhibitor, was chemically transformed into two biologically interesting compounds: the 4-epimer **2**, β-*galacto*-type *N*-octyl-valienamine, and the 4-*O*-(β-D-galactopyranosyl) derivative **3**, a carba-lactosylceramide analogue. The former, interestingly, could be demonstrated to act as a very effective inhibitor ($IC_{50}=0.3$ μM) of human β-galactosidase. The latter exhibited moderate inhibitory activity ($IC_{50}=20$ μM) against β-glucocerebrosidase (mouse liver).

Introduction

We previously reported that, among six *N*-alkyl[1] and six *N,N*-dialkyl-β-valienamines,[2] prepared in continuation of a chemical-modification program, the *N*-octyl derivative **1** exerts the strongest inhibition ($IC_{50}=0.03$ μM) of β-glucocerebrosidase (mouse liver). Since the glucosylceramide analogue composed of unsaturated 5a-carba-β-D-glucopyranose residue has been shown to be a strong and specific β-glucocerebrosidase inhibitor,[3] *N*-octyl β-valienamine having a β-*galacto* configuration, by analogy would be expected to show strong activity against β-galactocerebrosidase. This possibility was therefore examined in the present study. Furthermore, incorporation of a β-galactopyranose residue at C-4 of **1** was attempted to generate a lactosylceramide analogue, as a candidate[4] exo-β-galactoceramidase inhibitor.

Results and Discussion

The secondary amino function of *N*-octyl-2,3:4,6-di-*O*-isopropylidene-β-valienamine[1] (**4**) was first protected to give the *N*-*tert*-butoxycarbonyl derivative[5] (**5**), the isopropylidene groups of which were then removed with aqueous acetic acid (Fig. 1). The crude tetrol was then treated with α,α-dimethoxytoluene in DMF to give the 4,6-*O*-benzylidene derivative (**7**), which was further protected with methoxymethyl ether groups (→**8**). The benzylidene group was then removed and the resulting 6-hydroxyl group was selectively silylated to give the *tert*-butyldimethylsilyl derivative (**9**). The remaining free 4-hydroxyl group was then oxidized with pyridinium chlorochromate in CH_2Cl_2 and the resulting α,β-unsaturated ketone was reduced with 1 M lithium tri-*sec*-butyl borohydride in THF at −78 °C to give almost selectively the epimeric alcohol **10** in 66% yield. The ^1H NMR spectrum of **9** indicated a doublet of doublets ($J=9.9$ and 7.9 Hz) at δ 3.53, attributable to 3-H, whereas, in the spectrum of **10**, the signal due to 3-H appeared as a narrow doublet of doublets ($J=10.0$ and 2.0 Hz) at δ 3.46, confirming the structure proposed. This compound was finally deprotected by treatment with a mixture of 4 M hydrochloric acid and THF at 65 °C to afford, after purification over a column of Dowex 50W×2 (H^+) resin with 1% ammonia, to give *N*-octyl β-*galacto*-valienamine **2** in 91% yield.

For fear of difficulty of removal of the *N*-protecting group in the presence of an acid-labile glycoside linkage, a *N*-trifluoroacetyl group was selected for protection of compound **4**. The *N*-trifluoroacetyl derivative **6** was

*Corresponding author. Tel.: +81-45-566-1559; fax: +81-45-566-1551; e-mail: ogawa@applc.keio.ac.jp

0968-0896/02/$ - see front matter
PII: S0968-0896(02)00005-6

obtained quantitatively by treatment with trifluoroacetic anhydride in pyridine (Schemes 1 and 2). Compound **11**, obtained by similar deprotection of **6** followed by benzylidenation, was first treated with 6 molar equivalent of benzoyl chloride in pyridine at room temperature to yield the dibenzoate **12**, which, after removal of the benzylidene group, subjected to a selective benzoylation of the primary hydroxyl group with 1.5 molar equivalent of the reagent at −15 °C, affording the 2,3,6-tribenzoate **13** in 97% overall yield. Incorporation of a β-galactose residue at C-4 was effected, however, in a poor yield by coupling **13** with 3 molar equivalent of 2,3,4,6-tetra-*O*-acetyl-α-D-galactopyranosyl trichloroacetimidate[6,7] in dichloromethane in the presence of BF_3 etherate at 0 °C to room temperature, affording a carba-disaccharide derivative **14** in 19% yield, together with **13** (58%) recovered. The product was treated with methanolic potassium carbonate for 1h at room temperature to give, after purification by a resin column as in the preparation of **2**, free *N*-octyl-5a′-carba-β-lactosylamine **3** in 73% yield. The structure was established on the basis of the ^{1}H NMR spectrum.

Biological Assay

Biological assays of compound **2** (Table 1) showed[9] medium inhibitory activity ($IC_{50} = 5.0 \times 10^{-6}$ M) toward β-galactocerebrosidase (mouse liver). Interestingly, it was also demonstrated to possess strong activity ($IC_{50} = 3 \times 10^{-7}$ M) against β-galactosidase (human).[8] Therefore, chemical modification of **2** as a lead compound has been carried out extensively in our laboratory. We expect that the compounds of this group with a potent inhibitory activity against human β-galactosidase will be used in the near future for a new therapeutic trial of genetic β-galactosidase deficiency disorders as suggested in a previous report for Fabry disease with α-galactosidase deficiency.[4]

Table 1. Inhibitory activity (%) of compund **2** against β-galactosidase (human)

Inhibitor concentration (μm)	β-Galactoside activity (%)
0.000	100
0.050	77
0.125	60
0.250	43
0.500	36
1.000	36
2.500	19
5.000	14

Compound **3** was found to possess inhibitory activity ($IC_{50} = 2 \times 10^{-5}$ M) only against β-glucocerebrosidase (mouse liver).[3] The above results might be understood in terms of its original potential and/or formation of the strong inhibitor, *N*-octyl-β-valienamine, generated by partial enzymatic hydrolysis of **3**.

Experimental

General methods

Melting points were determined on a MEL-TEMP capillary melting point apparatus and are uncorrected. Optical rotations were measured with a JASCO DIP-370 polarimeter. Silica gel column chromatography was performed on silica gel 200–300 mesh (Wakogel C-300, Wako Junyaku Kogyo Co., Osaka), and analytical TLC on silica-gel 60 F-254 (E. Merck, Darmstadt). ^{1}H NMR spectra (270 and 300 MHz) were recorded on JEOL GSX-270 or JEOL GSX-300 instruments. Chemical shifts are expressed as δ values with reference to Me_4Si (δ 0.00) in $CDCl_3$, methanol-d_4, and DMSO-d_6, respectively. IR spectra were recorded on JASCO IR-810 of Hitachi FTS-65 spectrometers. Solutions were dried over anhydrous Na_2SO_4 and concentrated at <45 °C under diminished pressure.

***N*-Octyl-*N*-*tert*-butoxycarbonyl-2,3:4,6-di-*O*-isopropylidene-5a-carba-β-D-*xylo*-hex-5(5a)-enopyranosylamine (5).** To a solution of *N*-octyl-2,3:4,6-di-*O*-isopropylidene-5a-carba-β-D-*xylo*-hex-5(5a)-enopyranosylamine[1] (**4**, 644 mg, 1.75 mmol) in dichloromethane (13 mL) were added triethylamine (0.97 mL) and di-*tert*-butyldicarbonate (0.81 mL, 3.50 mmol), and the mixture was stirred at 25 °C. After 1.5 h, similar amounts of the reagents were again added and stirring continued for 1h. The mixture was diluted with ethyl acetate (180 mL), washed with saturated aqueous sodium hydrogen carbonate (60 mL) and brine (2×60 mL), dried, and evaporated. The residual product was purified by silica gel chromatography (50 g, EtOAc:hexane, gradient elution 1:11→1:8) to give **5** (807 mg, 99%) as a syrup, $[\alpha]_D^{22}$ −61° (*c* 0.90; $CHCl_3$); IR (neat) ν 1695 cm^{-1}; ^{1}H NMR [300 MHz, $(CD_3)_2SO$, 110 °C] δ 5.22 (br s, 1H, 5a-H), 4.59 (br d, 1H, $J_{3,4} = 9.3$ Hz, 4-H), 4.57 (br d, 1H, $J_{1,2} = 9.3$ Hz, 1-H), 4.40 and 4.13 (2 d, each 1H, $J_{gem} = 13.7$ Hz, 6,6-H), 3.74 (dd, 1H, $J_{2,3} = 9.3$ Hz, 2-H), 3.59 (dd, 1H, 3-H), 3.11 and 2.93 (2 m, each 1H, NCH_2), 1.54–1.18 (m, 12H, 6×CH_2), 1.47, 1.37, 1.36, and 1.29 (4 s, each 3H, 2×CMe_2), 1.40 (s, 9H, *t*-Bu), 0.86 (t, 3H, $J = 6.6$ Hz, CH_2CH_3). Anal. calcd for $C_{26}H_{45}NO_6$: C, 66.78; H, 9.70; N, 3.00. Found: C, 66.57; 10.10; N, 3.11.

***N*-Octyl-*N*-*tert*-butoxycarbonyl-4,6-*O*-benzylidene-5a-carba-β-D-*xylo*-hex-5(5a)-enopyranosylamine (7).** A mixture of **5** (768 mg, 1.64 mmol) and aqueous 60% acetic acid (16 mL) was stirred for 30 min at 60 °C, and then concentrated. The residue was co-evaporated with ethanol several times and eluted from a silica gel column (50 g, EtOH/toluene, gradient elution 1:10→1:4) to give a crude tetrol (540 mg) as a syrup. To a solution of a 242 mg-portion (0.62 mmol) of this compound in DMF (6 mL) were added α,α-dimethoxytoluene (112 μL, 0.75 mmol) and *p*-toluenesulfonic acid monohydrate (12 mg, 0.06 μmol), and the mixture was stirred for 3.5 h at 45 °C under diminished pressure provided by a water aspirator. Additional α,α-dimethoxytoluene (50 μL, 0.33 mmol) was then introduced, and the stirring continued for 2 h. The mixture was diluted with ethyl acetate (60 mL), washed with water and saturated aqueous sodium hydrogen carbonate, dried, and evaporated.

Formation of two products was detected by TLC (R_f 0.33 and 0.74 in acetone/toluene, 1:5; R_f 0.05 and 0.70 in EtOAc/toluene, 1:5). The residue was purified by silica gel chromatography (16 g, EtOAc/toluene, gradient elution 1:24→1:3) to give, first, the di-*O*-benzylidene compound (159 mg, 45%), and then **7** (164 mg, 55%) as a syrup. The former compound was dissolved in methanol (5 mL) and treated with *p*-toluenesulfonic acid monohydrate (3 mg) for 10 min at 0 °C. After neutralization with a drop of triethylamine, the mixture was evaporated and the residue was eluted from a silica gel column (7 g) with acetone:toluene (1:7) to give **7** (110 mg, combined yield 82%). $[\alpha]_D^{22}$ −57° (*c* 0.97, $CHCl_3$); IR (neat) ν 3420, 1695 cm^{-1}; ^1H NMR [300 MHz, $(CD_3)_2SO$, 110 °C] δ 7.46–7.27 (m, 5H, Ph), 5.65 (s, 1H, C*H*Ph), 5.31 (br s, 1H, 5a-H), 4.39 (br s, 2H, 6,6-H), 4.36 (br d, 1H, $J_{3,4}$ = 7.6 Hz, 4-H), 4.16 (br s, 1H, 1-H), 3.64 (dd, 1H, $J_{1,2} = J_{2,3}$ = 9.3 Hz, 2-H), 3.52 (dd, 1H, 3-H), 3.25–2.80 (m, 2H, NCH_2), 1.57–1.17 (m, 12H, 6× CH_2), 1.39 (s, 9H, CMe_3), 0.87 (t, 3H, J = 6.2 Hz, CH_2CH_3). Anal. calcd for $C_{27}H_{41}NO_6 \cdot 0.5H_2O$: C, 66.92; H, 8.73; N, 2.89. Found: C, 66.94; H, 8.85; N, 2.91.

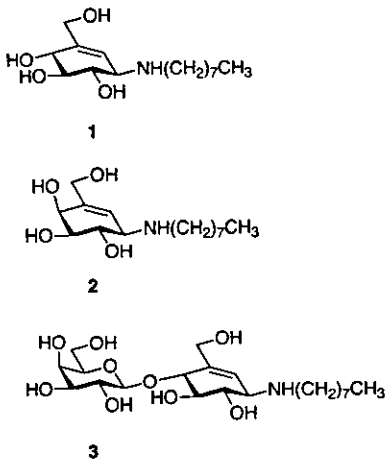

Figure 1.

***N*-Octyl-*N*-*tert*-butoxycarbonyl-4,6-*O*-benzylidene-2,3-di-*O*-methoxymethyl-5a-carba-β-D-*xylo*-hex-5(5a)-enopyranosylamine (8).** To a solution of **7** (269 mg, 0.566 mmol) in 1,2-dichloroethane (7 mL) were added chloromethyl ether (0.43 mL, 5.66 mmol) and *N*,*N*-diisopropylethylamine (1.97 mL, 11.3 mmol), and the mixture was stirred for 3 h at 60 °C. After dilution with chloroform (60 mL), the solution was washed with 1 M hydrochloric acid, saturated aqueous sodium hydrogen carbonate, and water, dried, and evaporated. The residue was purified by silica gel chromatography (20 g, EtOAc/toluene, gradient elution 1:14 → 1:9) to give **8** (315 mg, 99%) as a syrup: IR (neat) ν 1695 cm^{-1}; ^1H NMR [300 MHz, $(CD_3)_2SO$, 110 °C] δ 7.45–7.28 (m, 5H, Ph), 5.70 (s, 1H, C*H*Ph), 5.38 (br s, 1H, 5a-H), 4.79 and 4.77 (2 d, each 1H, J_{gem} = 6.1 Hz) and 4.75 and 4.63 (2 d, each 1H, J_{gem} = 6.3 Hz) (2 × OCH_2), 4.57 (br d, 1H, $J_{3,4}$ = 7.7 Hz, 4-H), 4.43 (br s, 2H, 6,6-H), 4.27 (br s, 1H, 1-H), 3.99 (dd, 1H, $J_{1,2}$ = 9.3, $J_{2,3}$ = 10.0 Hz, 2-H), 3.78 (dd, 1H, 3-H), 3.28 and 3.27 (2 s, each 3H, 2× OMe), 3.07–2.87 (m, 2H, NCH_2), 1.62–1.20 (m, 12H, 6× CH_2), 1.39 (s, 9H, *t*-Bu), 0.87 (t, 3H, J = 6.5 Hz, CH_2CH_3). Anal. calcd for $C_{31}H_{49}NO_8$: C, 66.05;H, 8.76; N, 2.48. Found: C, 65.80;H, 8.99; N, 2.42.

***N*-Octyl-*N*-*tert*-butoxycarbonyl-2,3-di-*O*-methoxymethyl-6-*O*-*tert*-butyldimethylsilyl-5a-carba-β-D-*xylo*-hex-5(5a)-enopyranosylamine (9).** A solution of **8** (315 mg, 0.56 mmol) and aqueous 60% acetic acid (8 mL) was stirred for 2 h at 60 °C, and concentrated. The residue was co-evaporated several times with ethanol and toluene, and then chromatographed on a silica gel column (20 g). Gradient elution with acetone/toluene (1:6 to 1:5) gave the diol (220 mg) as a syrup. A 160-mg-portion of this compound was dissolved in DMF (5 mL), to which *tert*-butylchlorodimethylsilane (100 mg, 0.67 mmol) was added. The mixture was stirred for 1h at room temperature, and then diluted with ethyl acetate (60 mL). The solution was washed with water, dried, and evaporated. The residual compound was purified by silica gel chromatography (20 g, EtOAc/toluene, 1:6) to give **9**

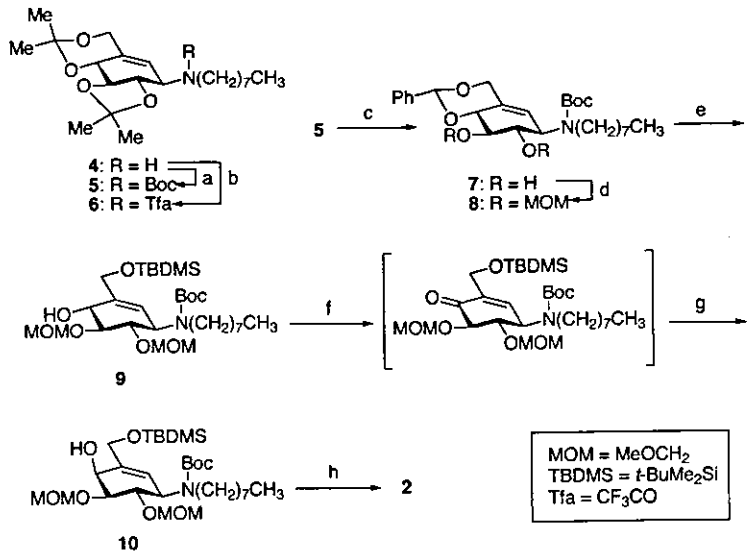

Scheme 1. Reagents and conditions: (a) $(t\text{-BuOCO})_2O$, Et_3N, CH_2Cl_2, rt; (b) $(CF_3CO)_2O$, pyridine, rt; (c) 60% aq AcOH, 60 °C; $PhCH(OMe)_2$, TsOH, DMF, 45 °C; (d) $MeOCH_2Cl$, $ClCH_2CH_2Cl$, $i\text{-Pr}_2EtN$, 60 °C; (e) 60% aq AcOH, 60 °C; $t\text{-BuMe}_2SiCl$, DMF, rt; (f) PCC, CH_2Cl_2, rt; (g) $s\text{-Bu}_3LiBH$, THF, −78 °C→0 °C; (h) 4 M HCl, THF, 65 °C; Dowex 50×2 (H^+) resin, 1% NH_3/MeOH.

(194 mg, 98%) as a syrup; $[\alpha]_D^{23}$ −101° (*c* 0.95, $CHCl_3$); IR (neat) ν 3445 (OH), 1695 (amide) cm^{-1}; ^1H NMR [300 MHz, $(CD_3)_2SO$, 110 °C] δ 5.36 (br s, 1H, 5a-H), 4.83 and 4.76 (2 d, each 1H, J_{gem} = 6.1 Hz), and 4.73 and 4.60 (2 d, each 1H, J_{gem} = 6.3 Hz) (2×OCH_2), 4.21 and 4.11 (ABq, J_{gem} = 13.9 Hz, 6,6-H), 4.12–4.04 (m, 2H, 1-H, 4-H), 3.87 (dd, 1H, $J_{1,2}$ = 9.3, $J_{2,3}$ = 9.9 Hz, 2-H), 3.53 (dd, 1H, $J_{3,4}$ = 7.9 Hz, 3-H), 3.35 and 3.26 (2 s, each 3H, 2×OCH_3), 3.05–2.88 (m, 2H, NCH_2), 1.60–1.20 (m, 12H, 6×CH_2), 1.38 (s, 9H, $OCMe_3$), 0.89 (s, 9H, $CCMe_3$), 0.86 (t, 3H, *J* = 6.8 Hz, CH_2CH_3), 0.05 (s, 6H, $SiMe_2$). Anal. calcd for $C_{30}H_{59}NO_8Si$: C, 61.08;H, 10.08; N, 2.37. Found: C, 60.82;H, 10.38; N, 2.45.

***N*-Octyl-*N*-*tert*-butoxycarbonyl-2,3-di-*O*-methoxymethyl-6-*O*-*tert*-butyldimethylsilyl-5a-carba-α-L-*arabino*-hex-5(5a)-enopyranosylamine (10).** To a solution of compound **9** (75 mg, 0.13 mmol) in CH_2Cl_2 (2 mL) were added powdered 4 A molecular sieves (75 mg) and pyridinium chlorochromate (41 mg, 0.19 mmol), and the mixture was stirred for 1h at room temperature. Additional pyridinium chlorochromate (41 mg, 0.19 mmol) was added, and stirring continued for 1h. The mixture was filtered through a Celite bed and the filtrate was chromatographed on a short column of silica gel with diethyl ether as an eluent to give a crude ketone. This compound was dissolved in THF (0.7 mL) and the solution was treated with 1 M lithium tri-*s*-butyl borohydride/THF solution (0.51 mL, 0.51 mmol) under argon for 30 min at −78 °C. The reaction mixture was allowed to warm to 0 °C and the reaction was quenched by addition of saturated aqueous ammonium chloride. After addition of magnesium sulfate, the solution was filtered through a Celite bed and the filtrate was evaporated. The crude product was purified by silica gel chromatography (7 g, EtOAc:toluene, gradient elution 1:9→1:6) to give **10** (49 mg, 66%) as a syrup; $[\alpha]_D^{23}$ −68° (*c* 1.13, $CHCl_3$); IR (neat) ν 3460 (OH), 1695 (amide) cm^{-1}; ^1H NMR [300 MHz, $(CD_3)_2SO$, 110 °C] δ 5.36 (br s, 1H, 5a-H), 4.71 and 4.59 (2 d, each 1H, J_{gem} = 5.6 Hz) and 4.75–4.66 (m, 2H) (2 × OCH_2), 4.38 (br s, 1H, 1-H), 4.19 and 4.12 (2 d, each 1H, J_{gem} = 13.2 Hz, 6,6-H), 4.13–4.02 (m, 2H, 2-H, 4-H), 3.46 (dd, 1H, $J_{2,3}$ = 10.3, $J_{3,4}$ = 2.0 Hz, 3-H), 3.33 and 3.25 (2 s, each 3H, 2 × OMe), 3.10–2.86 (m, 2H, 1′,1′-H), 1.62–1.16 (m, 12H, 6 × CH_2), 1.39 (s, 9H, $CCMe_3$), 0.89 (s, 9H, $SiCMe_3$), 0.86 (t, 3H, *J* = 7.3 Hz, CH_2CH_3), 0.05 (s, 6H, $SiMe_2$). Anal. calcd for $C_{30}H_{59}NO_8Si$: C, 61.08;H, 10.08; N, 2.37. Found: C, 60.80;H, 10.37; N, 2.53.

***N*-Octyl-5a-carba-α-L-*arabino*-hex-5(5a)-enopyranosylamine (2).** A solution of **10** (29 mg, 0.049 mmol) in a mixture of THF (0.5 mL) and 4 M hydrochloric acid (1.5 mL) was stirred for 1.5 h at 65 °C, and then evaporated and co-evaporated with ethanol. The product was purified over a Dowex-50W×2 (H^+) resin column with 1% methanolic ammonia as an eluent to give **2** (13 mg, 91%) as a white solid: mp 126–128 °C; R_f 0.76 (MeOH:$CHCl_3$:H_2O, 35:60:5); $[\alpha]_D^{23}$ +16° (*c* 0.64, MeOH); IR (KBr) ν 3485 (OH), 3250 (amine) cm^{-1}; ^1H NMR (300 MHz, $CD_3OD/CDCl_3$, 1:2) δ 5.73 (d, 1H, $J_{1,5a}$ = 1.8 Hz, 5a-H), 4.16 (d, 1H, $J_{3,4}$ = 4.2 Hz, 4-H), 4.16 (br. s, 2H, 6,6-H_2), 3.64 (dd, 1H, $J_{1,2}$ = 8.1, $J_{2,3}$ = 10.0 Hz, 2-H), 3.48 (dd, 1H, 3-H), 3.12 (dd, 1H, 1-H), 2.78 (ddd, 1H, $J_{1'a,2'}$ = 7.4, J_{gem} = 11.2 Hz) and 2.57 (ddd, 1H) (NCH_2), 1.64–1.21 (m, 12H, 6 × CH_2), 0.89 (t, 3H, *J* = 6.7 Hz, CH_2CH_3). Anal. calcd for $C_{15}H_{29}NO_4$: C, 62.69;H, 10.17; N, 4.87. Found: C, 62.67;H, 10.47; N, 5.01.

***N*-Octyl-*N*-trifluoroacetyl-2,3:4,6-di-*O*-isopropylidene-5a-carba-β-D-*xylo*-hex-5(5a)-enopyranosylamine (6).** To a solution of **4** (2.60 g, 7.07 mmol) in pyridine (40 mL) was added trifluoroacetic anhydride (2.0 mL, 14 mmol), and the mixture was stirred for 1h at room temperature and then evaporated. The residue was dissolved in ethyl acetate (360 mL) and the solution was washed with water, dried, and evaporated. The product was purified by silica gel chromatography (150 g, EtOAc:hexane, 1:10) to give **6** (3.26 g, 99%) as a colorless syrup; $[\alpha]_D^{30}$ −72° (*c* 1.20, $CHCl_3$); IR (neat) ν 1695 (amide) cm^{-1}; ^1H NMR [300 MHz, $(CD_3)_2SO$, 110 °C] δ 5.30 (br s, 1H, 5a-H), 4.79–4.61 (m, 2H, 1-H, 4-H), 4.43 and 4.16 (2 d, each 1H, J_{gem} = 13.9 Hz, 6,6-H), 3.86 (br s, 1H, 2-H), 3.72 (dd, 1H, $J_{2,3}$ = 8.3, $J_{3,4}$ = 7.8 Hz, 3-H), 3.33 and 3.12 (2 m, 1H, NCH_2), 1.67–1.17 (m, 12H, 6 × CH_2), 1.49, 1.38, 1.30, and 1.27 (4 s, each 3H, 2 × CMe_2), 0.86 (t, 3H, *J* = 7.1 Hz, CH_2CH_3). Anal. calcd for $C_{23}H_{36}F_3NO_5$: C, 59.60;H, 7.83; N, 3.02. Found: C, 59.79;H, 7.79; N, 2.96.

***N*-Octyl-*N*-trifluoroacetyl-4,6-*O*-benzylidene-5a-carba-β-D-*xylo*-hex-5(5a)-enopyranosylamine (11).** A solution of **6** (3.08 g, 6.64 mmol) and aqueous 80% acetic acid (50

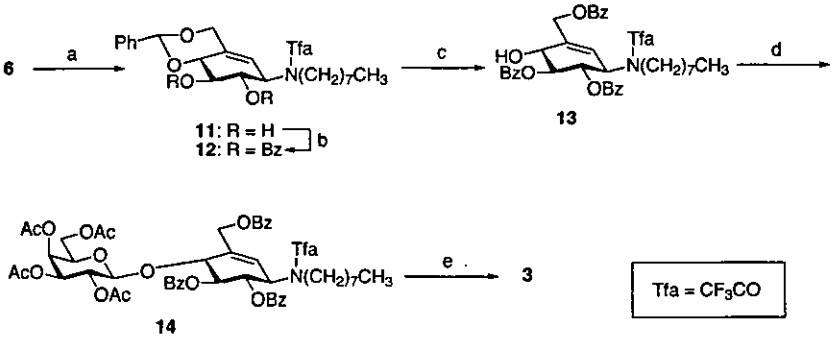

Scheme 2. Reagents and conditions: (a) 80% aq AcOH, 80 °C; $PhCH(OMe)_2$, TsOH, DMF, 45 °C; (b) BzCl (6 mol equiv), pyridine, rt; (c) 80% aq AcOH, 80 °C; BzCl (1.5 mol equiv), pyridine, −15 °C; (d) 2,3,4,6-tetra-*O*-acetyl-β-D-galactopyranosyl trichloroacetimidate (3 mol equiv), BF_3/diethyl ether, molecular sieves 4 A, CH_2Cl_2, 0 °C, 0.5 h; (e) aq K_2CO_3, 1H, rt; Dowex 50 × 2 (H^+) resin, 1% NH_3/MeOH.

mL) was stirred for 30 min at 80 °C. The residue was concentrated and co-evaporated with ethanol three times and then with toluene. The residual product was dissolved in DMF (40 mL), to which were added α,α-dimethoxytoluene (2.0 mL, 13 mmol) and *p*-toluenesulfonic acid monohydrate (130 mg, 0.67 mmol). The mixture was stirred for 2 h at 45 °C under diminished pressure (water aspirator). The mixture was diluted with ethyl acetate (330 mL) and the solution was washed with water, saturated aqueous sodium hydrogen carbonate, dried, and evaporated. The products (R_f 0.15 and 0.83, EtOAc:toluene, 1:5) were chromatographed on a silica gel column (150 g) with EtOAc:toluene (gradient elution 1:7→1:6) to give **11** (1.96 g, 63%) as a syrup, together with a mixture (1.58 g, 37%) of isomeric di-*O*-benzylidene derivatives. A 1.5 g portion of the latter was dissolved in methanol (50 mL) and treated with *p*-toluenesulfonic acid monohydrate (47 mg) at 0 °C. After 10 min, the mixture was neutralized with triethylamine and evaporated. The residue was purified on a silica gel column (30 g, EtOAc:toluene, 1:6) to give **11** (0.93 g, 30%); $[\alpha]_D^{29}$ −78° (*c* 1.1, $CHCl_3$); IR (neat) ν 3440 (OH), 1695 (amide) cm^{-1}; ^1H NMR [300 MHz, $(CD_3)_2SO$, 150 °C] δ 7.48–7.27 (m, 5H, Ph), 5.68 (s, 1H, C*H*Ph), 5.38 (br s, 1H, 5a-H), 4.49–4.34 (m, 4H, 1-H, 4-H, 6,6-H), 3.77 (br s, 1H, 2-H), 3.60 (dd, 1H, $J_{2,3}$ = 9.5, $J_{3,4}$ = 7.6 Hz, 3-H), 3.50–3.05 (m, 2H, NCH_2), 1.61–1.21 (m, 12H, 6 × CH_2), 0.87 (t, 3H, J = 6.5 Hz, CH_2CH_3). Anal. calcd for $C_{24}H_{32}F_3NO_5$: C, 61.13;H, 6.84; N, 2.97. Found: C, 61.06;H, 6.83; N, 2.97.

***N*-Octyl-*N*-trifluoroacetyl-2,3-di-*O*-benzoyl-4,6-*O*-benzylidene-5a-carba-β-D-*xylo*-hex-5(5a)-enopyranosylamine (12).** A solution of **11** (1.88 g, 3.99 mmol) in pyridine (30 mL) was treated with benzoyl chloride (2.77 mL, 23.9 mmol) for 5 h at room temperature. The mixture was then diluted with ethyl acetate (230 mL) and the solution was thoroughly washed with water, dried, and evaporated. The residue was purified by silica gel chromatography (200 g, EtOAc:hexane, gradient elution 1:9→1:6) to give **12** (2.69 g, 99%) as a white solid; mp 173–175 °C; $[\alpha]_D^{23}$ −69° (*c* 1.1, $CHCl_3$); IR (neat) ν 3460 (OH), 1730 (ester), 1695 (amide) cm^{-1}; ^1H NMR [300 MHz, $(CD_3)_2SO$, 150 °C] δ 7.95–7.26 (m, 15H, 3×Ph), 6.00 (br s, 1H, 2-H), 5.78 (dd, 1H, $J_{2,3}$ = 10.7, $J_{3,4}$ = 7.8 Hz, 3-H), 5.78 (s, 1H, C*H*Ph), 5.70 (br s, 1H, 5a-H), 5.10 (br d, 1H, 4-H), 5.02 (br d, 1H, $J_{1,2}$ = 7.8 Hz, 1-H), 4.58 (br s, 2H, 6,6-H), 3.52 and 3.31 (2 m, each 1H, NCH_2), 1.70–1.18 (m, 12H, 6×CH_2), 0.85 (t, 3H, J = 6.8 Hz, CH_2CH_3). Anal. calcd for $C_{38}H_{40}F_3NO_7$: C, 67.15;H, 5.93; N, 2.06. Found: C, 67.12;H, 5.93; N, 2.00.

***N*-Octyl-*N*-trifluoroacetyl-2,3,6-tri-*O*-benzoyl-5a-carba-β-D-*xylo*-hex-5(5a)-enopyranosylamine (13).** A solution of **12** (2.63 g, 3.87 mmol) and aqueous 80% acetic acid (85 mL) was stirred for 1.5 h at 80 °C, and then concentrated. The residue was co-evaporated with ethanol and toluene. The product was dissolved in pyridine (45 mL), to which benzoyl chloride (0.67 mL, 5.8 mmol) was added at −15 °C, and the mixture was stirred for 2 h at −15 °C. It was then diluted with ethyl acetate (300 mL), and the solution was thoroughly washed with water, dried, and evaporated. The product was purified by column chromatography (150 g, EtOAc:toluene, 1:15) to give **13** (2.61 g, 97%) as a syrup; R_f 0.56 (EtOAc:toluene, 1:5); $[\alpha]_D^{23}$ −29° (*c* 0.95, $CHCl_3$); IR (neat) ν 1730 (ester), 1695 (amide) cm^{-1}; ^1H NMR [300 MHz, $(CD_3)_2SO$, 150 °C] δ 8.03–7.30 (m, 15H, 3×Ph), 5.87 (br s, 1H, 2-H), 5.76 (br s, 1H, 5a-H), 5.57 (dd, 1H, $J_{2,3}$ = 9.8, $J_{3,4}$ = 8.1 Hz, 3-H), 5.07–4.98 (m, 1H, 1-H), 5.03 and 4.92 (2 d, each 1H, J_{gem} = 12.9 Hz, 6,6-H), 4.74 (br d, 1H, 4-H), 3.37–3.27 (m, 2H, NCH_2), 1.62–1.12 (m, 12H, 6×CH_2), 0.83 (t, 3H, J = 6.3 Hz, CH_2CH_3). Anal. calcd for $C_{38}H_{40}F_3NO_8$: C, 65.60;H, 5.80; N, 2.01. Found: C, 65.68;H, 5.78; N, 2.05.

***N*-Octyl-*N*-trifluoroacetyl-4-*O*-(2,3,4,6-tetra-*O*-acetyl-β-D-galactopyranosyl)-2,3,6-tri-*O*-benzoyl-5a-carba-β-D-*xylo*-hex-5(5a)-enopyranosylamine (14).** To a stirred mixture of **13** (94 mg, 0.135 mmol), 2,3,4,6-tetra-*O*-acetyl-β-D-galactopyranosyl trichloroacetimidate[5] (200 mg, 0.406 mmol) and powdered 4 A molecular sieves (100 mg) in dichloromethane (2 mL) was added 47% trifluoroborane etherate (110 μL, 0.41 mmol) at 0 °C under argon. The mixture was stirred for 30 min at room temperature, then neutralized with sodium hydrogen carbonate, and filtered through a Celite bed. The filtrate was diluted with ethyl acetate (60 mL) and the solution was washed with saturated aqueous sodium hydrogen carbonate and brine, dried, and evaporated. The residual products were purified by column chromatography on silica gel (27 g, EtOAc/toluene, gradient elution 1:11→1:9) to give **14** (26 mg, 19%) as a syrup, together with **13** (54 mg, 58%); R_f 0.18 (AcOH:toluene, 1:5); $[\alpha]_D^{23}$ −43° (*c* 1.1, $CHCl_3$); IR (neat) ν 1730 (ester), 1695 (amide) cm^{-1}; ^1H NMR [300 MHz, $(CD_3)_2SO$, 110 °C] δ 8.07–7.27 (m, 15H, 3×Ph), 6.04–5.84 (m, 1H, 2-H), 5.93 (br s, 1H, 5a-H), 5.74 (dd, 1H, $J_{2,3}$ = 8.8, $J_{3,4}$ = 8.1 Hz, 3-H), 5.11–4.81 (m, 8H, 1-H, 4-H, 6,6-H, 1′-H, 2′-H, 3′-H, 4′-H), 4.01–3.22 (m, 3H, 5′-H, 6′,6′-H), 3.40–3.22 (m, 2H, NCH_2), 2.00, 1.92, 1.87, and 1.85 (4 s, each 3H, 4×Ac), 1.60–1.03 (m, 12H, 6×CH_2), 0.82 (t, 3H, J = 6.5 Hz, CH_2CH_3). Anal. calcd for $C_{52}H_{58}F_3NO_{17}$: C, 60.87;H, 5.70; N, 1.37. Found: C, 60.44;H, 5.56; N, 1.41.

4-*O*-(β-D-Galactopyranosyl)-*N*-octyl-5a-carba-β-D-*xylo*-hex-5(5a)-enopyranosylamine (3). To a solution of **14** (26 mg, 0.025 mmol) in methanol (2 mL) was added potassium carbonate (60 mg, 0.43 mmol), and the mixture was stirred for 1h at room temperature. The mixture was taken up on a column of Dowex 50W×2 (H^+) resin and eluted with 1% methanolic ammonia to give **3** (11 mg, 73%) as a white solid; R_f 0.34 (MeOH:$CHCl_3$:H_2O, 35:60:8); $[\alpha]_D^{23}$ −65° (*c* 0.44, MeOH); IR (KBr) ν 3440 (OH) cm^{-1}; ^1H NMR (270 MHz, CD_3OD/$CDCl_3$, 1:2) δ 5.62 (br s, 1H, 5a-H), 4.43 (d, $J_{1',2'}$ = 7.3 Hz, 1′-H), 4.34 and 4.02 (2 d, each 1H, J_{gem} = 13.4 Hz, 6,6-H), 4.25 (br d, 1H, $J_{3,4}$ = 7.7 Hz, 4-H), 3.92–3.47 (m, 5H, 3′-H, 4′-H, 5′-H, 6′,6′-H), 3.69 (dd, 1H, $J_{2,3}$ = 10.3 Hz, 3-H), 3.63 (dd, 1H, $J_{2',3'}$ = 9.5 Hz, 2′-H), 3.51 (dd, 1H, $J_{1,2}$ = 8.8, 2-H), 3.23 (br d, 1H, 1-H), 2.74 and 2.53 (ddd, each 1H, J = 7.3, J_{gem} = 11.4 Hz, NCH_2), 1.62–1.20 (m, 12H, 6×CH_2), 0.89 (t, 3H, J = 6.6 Hz, CH_2CH_3).

Biological assay

The knockout mouse fibroblasts[10] transformed by SV-40 cDNA and expressing human β-galactosidase were cultured in serum-free Dulbecco's modified Eagle's medium (DMEM) containing 10 mM NH_4Cl for 24 h.[11] The culture medium was collected, dialyzed against 10 mM phosphate buffer, pH 6.5, concentrated, and used for the inhibition experiment. The enzyme activity was assayed with 4-methylumbelliferyl β-galactopyranoside as substrate as reported previously[12] in the presence of varying amounts of the inhibitor.

Acknowledgements

The authors thank Mr. K. Kabayama for some of the preparative work, Mr. K. Hokazono for performing elementary analyses, and Drs. E. Nanba and L. Tominaga (Tottori University, Matsue, Japan) for some of the biological assays.

References and Notes

1. Ogawa, S.; Ashiura, M.; Uchida, C.; Watanabe, S.; Yamazaki, C.; Yamagishi, K.; Inokuchi, J. *Bioorg. Med. Chem. Lett.* **1996**, *6*, 929.
2. Ogawa, S.; Kobayashi, Y.; Kabayama, K.; Jimbo, M.; Inokuchi, J. *Bioorg. Med. Chem.* **1998**, *6*, 1955.
3. Tsunoda, H.; Inokuchi, J.; Yamagishi, K.; Ogawa, S. *Liebigs Ann. Chem.* **1995**, 279.
4. Fan, J.-Q.; Ishii, S.; Asano, N.; Suzuki, Y. *Nat. Med.* **1999**, *5*, 112.
5. The ^1H NMR spectra of a series of the *N*-protected derivatives described here appeared to be complex at room temperature, owing to restricted rotation of the *N*-alkoxycarbonyl-*N*-alkyl functions. In order to overcome the unfavorable circumstances, the collapsed spectra were measured in DMSO-d_6 at elevated temperature (>110 °C).
6. Amvam-Zollo, P. H.; Sinaÿ, P. *Carbohydr. Res.* **1986**, *150*, 199.
7. Later, 2,3,4,6-tetra-*O*-pivaloyl-α-D-galactopyranosyl trichloroacetimidate[8] has been shown to be a very effective donor in this coupling reaction, affording a 97% yield of the pseudo-disaccharide under similar reaction conditions. However, very interestingly, the coupling product appeared seemingly to be an α-glycoside, considering the ^1H NMR spectrum of the deprotected disaccharide: ^1H NMR (300 MHz, $CD_3OD/CDCl_3$, 1:2) (inter alia) $\delta = 3.23$ (br d, 1H, $J_{1,2} = \sim 9.0$ Hz, 1-H), 3.48 (dd, 1H, $J_{2,3} = 9.0$ Hz, 2-H), 5.14 (br s, 1H, 1′-H), 5.65 (br s, 1H, 5a-H).
8. Zimmermann, P. Dissertation, University of Konstanz, 1988.
9. The activity of compound **4** similarly corresponds with that of the derivative[3] having a ceramide chain. Free β-*galacto*-type valienamine did not show any inhibitory activity against galactocerebrosidase, as with the lack of effects β-valienamine (β-*gluco*-type) against glucocerebrosidase: Ogawa, S.; Kabayama, K. Unpublished results.
10. Matsuda, J.; Suzuki, O.; Oshima, A.; Ogura, A.; Noguchi, Y.; Yamamoto, Y.; Asano, T.; Tokimoto, K.; Sukegawa, K.; Suzuki, Y.; Naiki, M. *Glycoconjugate J.* **1997**, *14*, 729.
11. Tominaga, L.; Ogawa, Y.; Taniguchi, M.; Ohno, K.; Matuda, J.; Oshima, A.; Suzuki, Y.; Nanba, E. *Brain Dev.* **2001**, *23*, 284.
12. Sakuraba, H.; Aoyagi, T.; Suzuki, Y. *Clin. Chim. Acta* **1982**, *125*, 275.

Chemical chaperone therapy for brain pathology in G_{M1}-gangliosidosis

Junichiro Matsuda*, Osamu Suzuki*, Akihiro Oshima*, Yoshie Yamamoto*, Akira Noguchi*, Kazuhiro Takimoto†, Masayuki Itoh‡, Yuji Matsuzaki§, Yosuke Yasuda§, Seiichiro Ogawa¶, Yuko Sakata¶, Eiji Nanba‖, Katsumi Higaki‖, Yoshimi Ogawa‖, Lika Tominaga‖, Kousaku Ohno**, Hiroyuki Iwasaki††, Hiroshi Watanabe††, Roscoe O. Brady‡‡, and Yoshiyuki Suzuki§§¶¶

*Department of Veterinary Science, and †Division of Experimental Animal Research, National Institute of Infectious Diseases, 1-23-1 Toyama, Shinjuku-ku, Tokyo 162-8640, Japan; ‡Department of Mental Retardation and Birth Defect Research, National Institute of Neuroscience, National Center of Neurology and Psychiatry, 4-1-1 Ogawa-Higashi, Kodaira, Tokyo 187-8502, Japan; §Central Research Laboratories, Seikagaku Corporation, 3-1253 Tateno, Higashi-Yamato, Tokyo 207-0021, Japan; ¶Department of Biosciences and Informatics, Faculty of Science and Technology, Keio University, 3-14-1 Hiyoshi, Kohoku-ku, Yokohama 223-8522, Japan; ‖Division of Functional Genomics, Research Center for Bioscience and Technology, Tottori University, 86 Nishi-machi, Yonago 683-8503, Japan; **Division of Child Neurology, Faculty of Medicine, Tottori University, 36-1 Nishi-machi, Yonago 683-8504, Japan; ††Nasu Institute for Developmental Disabilities, 2600-7 Kita-Kanemaru, Otawara 324-0011, Japan; ‡‡Developmental and Metabolic Neurology Branch, National Institute of Neurological Disorders and Stroke, National Institutes of Health, 9000 Rockville Pike, Bethesda, MD 20892-1260; and §§Clinical Research Center, International University of Health and Welfare, 2600-1 Kita-Kanemaru, Otawara 324-8501, Japan

Contributed by Roscoe O. Brady, October 15, 2003

We synthesized a galactose derivative, *N*-octyl-4-epi-β-valienamine (NOEV), for a molecular therapy (chemical chaperone therapy) of a human neurogenetic disease, β-galactosidosis (G_{M1}-gangliosidosis and Morquio B disease). It is a potent inhibitor of lysosomal β-galactosidase *in vitro*. Addition of NOEV in the culture medium restored mutant enzyme activity in cultured human or murine fibroblasts at low intracellular concentrations, resulting in a marked decrease of intracellular substrate storage. Short-term oral administration of NOEV to a model mouse of juvenile G_{M1}-gangliosidosis, expressing a mutant enzyme protein R201C, resulted in significant enhancement of the enzyme activity in the brain and other tissues. Immunohistochemical stain revealed a decrease in the amount of G_{M1} and G_{A1} in neuronal cells in the fronto-temporal cerebral cortex and brainstem. However, mass biochemical analysis did not show the substrate reduction observed histochemically in these limited areas in the brain probably because of the brief duration of this investigation. Chemical chaperone therapy may be useful for certain patients with β-galactosidosis and potentially other lysosomal storage diseases with central nervous system involvement.

Hereditary deficiency of lysosomal acid β-galactosidase (β-galactosidosis) causes two clinically distinct diseases in humans, G_{M1}-gangliosidosis and Morquio B disease (1). The mode of inheritance is autosomal recessive. G_{M1}-gangliosidosis is a generalized neurosomatic disease occurring mainly in early infancy, and rarely in childhood or young adults. Morquio B disease is a rare systemic bone disease without central nervous system involvement.

Glycoconjugates with terminal β-galactose residues accumulate in tissues and urine from patients with these clinical phenotypes. Ganglioside G_{M1} and its asialo derivative G_{A1} accumulate in the G_{M1}-gangliosidosis brain. High amounts of oligosaccharides derived from keratan sulfate or glycoproteins are detected in visceral organs and urine from G_{M1}-gangliosidosis and Morquio B disease patients.

At present only symptomatic therapy is available for human β-galactosidosis patients. Allogeneic bone marrow transplantation did not modify subsequent clinical course or cerebral enzyme activity in a Portuguese water dog affected with G_{M1}-gangliosidosis (2). Amniotic tissue transplantation was not effective in a patient with Morquio B disease (3). Enzyme replacement therapy conducted for Gaucher disease and other lysosomal storage diseases is not available at present for β-galactosidosis.

Recently we reported results of a molecular approach (chemical chaperone therapy) for restoration of mutant α-galactosidase in Fabry disease. Galactose and its structural analog, 1-deoxygalactonojirimycin, restored residual enzyme activity in cultured human lymphoblasts from patients with α-galactosidase deficiency (4, 5) and transgenic (Tg) mouse tissues expressing a mutant enzyme causing Fabry disease (5, 6). Some mutant proteins are unstable at neutral pH in the endoplasmic reticulum/Golgi apparatus and are rapidly degraded without appropriate molecular folding (7, 8). Certain exogenous compounds that inhibit enzyme activity *in vitro* bind to the enzyme intracellularly, resulting in the formation of a complex that stabilizes and transports the catalytically active enzyme to lysosomes. Under the acidic condition in lysosomes, the complex dissociates, and the mutant enzyme remains stabilized and functional.

In this study, we synthesized a compound for possible molecular therapy of brain pathology in β-galactosidosis and confirmed its restorative effect on the model mouse brain after short-term oral administration.

Materials and Methods

Synthesis of a β-Galactosidase Inhibitor, *N*-octyl-4-epi-β-valienamine (NOEV). We chemically modified a glucocerebrosidase inhibitor (Fig. 1*A*; compound **1**) (9–11) by replacing the ceramide moiety with simple aliphatic chains (11, 12) and multistep epimerization at C-4 (13). In this study, we chose an *N*-octyl derivative, *N*-octyl-4-epi-β-valienamine (Fig. 1*B*) for experimental studies of chemical chaperone therapy (5) in murine G_{M1}-gangliosidosis. We use the term NOEV as abbreviation of this compound. Its structure was assigned by a combination of COSY, total correlation spectroscopy (TOCSY), and heteronuclear sequential quantum correlation (HSQC) NMR spectroscopy. NMR spectra were recorded with a Varian UNITYINOVA 500 [^{1}H (500 MHz) or ^{13}C (125 MHz)] spectrometer. Chemical shifts were expressed in ppm downfiled from the signal for internal Me_4Si for solutions in CD_3OD. The sample temperature was 23°C, and concentration was 10 mg/ml.

Cell Culture and NOEV Experiments. Human and murine fibroblasts were cultured and used for enzyme inhibition/restoration experiments. Fibroblasts from human patients with G_{M1}-gangliosidosis or Morquio B disease were kindly provided by

Abbreviations: NOEV, *N*-octyl-4-epi-β-valienamine; KO, knockout; Tg, transgenic; X-Gal, 5-bromo-4-chloro-3-indolyl-β-D-galactopyranoside.

¶¶To whom correspondence should be addressed at: Clinical Research Center, Room L-423, International University of Health and Welfare, 2600-1 Kita-Kanemaru, Otawara 324-8501, Japan. E-mail: suzukiy@iuhw.ac.jp.

www.pnas.org/cgi/doi/10.1073/pnas.2536657100

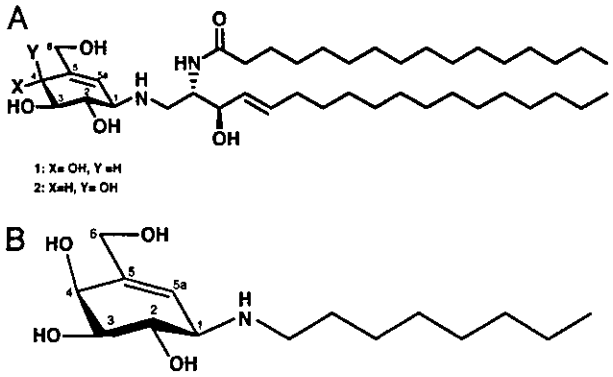

Fig. 1. Structure of inhibitors for β-glucosidase and β-galactosidase. (*A*) Synthetic derivatives of glucosylceramide (**1**) and galactosylceramide (**2**). (*B*) Structure of *N*-octyl-4-epi-β-valienamine (NOEV).

colleagues in Japan and other countries or purchased from Coriell Institute for Medical Research (Camden, NJ). Mouse fibroblast lines expressing mutant human β-galactosidase were established as reported (14). They were cultured in DMEM with 10% FCS and antibiotics. NOEV was added at various concentrations to the culture medium of fibroblasts from human patients or genetically engineered mice.

Ganglioside Loading of Cultured Mouse Fibroblasts. The mouse fibroblasts expressing wild-type (GP8) or R201C mutant human β-galactosidase were cultured in medium containing bovine ganglioside mixture (0.1 mg/ml; Sigma) for 2 days followed by culture in the presence of NOEV (0.2 μM) for 4 subsequent days. The cells were stained with FITC-labeled cholera toxin B (Sigma) to detect ganglioside G_{M1} (15).

Gene Mutation Analysis. We analyzed mutant genes as described (14). In short, after extraction of genomic DNA from human fibroblasts, each of 16 exons with flanking sequence was amplified by PCR under the standard conditions. All exons except 1, 4, 7, and 9 were sequenced directly by using ABI PRISM 3100 Genetic Analyzer (Applied Biosystems Japan, Tokyo, Japan). The amplified exons 1, 4, 7, and 9 were subjected to single strand conformation polymorphism (16). Exons with aberrant bands were subcloned into pGEM-T vector (Promega) and sequenced.

Knockout (KO) and KO-Tg Mice. We prepared a C57BL/6-based congenic strain KO mouse with β-galactosidase deficiency as reported (17). Then, we produced a Tg mouse line overexpressing mutant human β-galactosidase with an amino acid substitution R201C that causes juvenile type G_{M1}-gangliosidosis in humans by injecting the DNA fragment containing β-actin promoter (CAG promoter) and human mutant β-galactosidase cDNA (R201C) into C57BL/6 fertilized eggs. Cross-breeding of the KO mice and Tg mice was performed to obtain KO-Tg mice (R201C mice). We used hemizygous Tg mice with the β-galactosidase KO background in this study. Presence of the mutation of human β-galactosidase gene (R201C) in these mice was confirmed by DNA sequencing. We further confirmed that these mice expressed human β-galactosidase but did not express endogenous mouse enzyme by Northern blot analysis and RT-PCR. The genotype of these mice was determined by PCR amplification of tail DNA, using the following primer sets: 5′-GCTGGTTGTTGTGCTGTCTCATCATT-3′ (sense) and 5′-AGTTCCAGGGCACATACGTCTGGAT-3′ (antisense) for detection of human β-galactosidase transgene (PCR product, ≈330 bp); 5′-CTCGCGCCAGCCGAACTGTT-3′ (sense) and 5′-GTTCGAGGCCACACGCGTCA-3′ (antisense) for detection of neo^r gene (PCR product, 570 bp); and 5′-CATTCCTGCCAAGACAGTAG-3′ (sense) and 5′-ATGGCCTCAGTGTTCAGTGGG-3′ (antisense) for detection of wild-type exon 15 of mouse β-galactosidase gene (PCR product, 242 bp). PCR was performed by using *Taq* polymerase (EX-*Taq*, Takara, Ohtsu, Japan) at 30 cycles of reaction at 94°C for 30 s, 60°C for 30 s, and 72°C for 30 s. The care of experimental animals was carried out in accordance with the guidelines on animal experimentation of the National Institute of Infectious Diseases (Tokyo).

Oral Administration of NOEV to the R201C Mouse. An aqueous solution of NOEV (0.1–1 mM) was given ad libitum orally to the R201C mouse for 1 week. The mouse was anesthetized with ethylether; blood was collected by cardiac puncture, and then brain and other tissues were removed. The brain was immediately divided into two sagittal sections, one for biochemical analysis and the other for pathological analysis. For comparison with ad libitum oral administration of NOEV, we also analyzed mice to which daily doses of 0.5 ml of 1 mM NOEV were administered by gavage.

Histochemistry and Immunohistochemistry of Mouse Tissues. Brain tissue was immersed in 4% phosphate-buffered paraformaldehyde overnight and frozen for embedding in OTC (optimal cutting temperature) compound (Sakura Finetechnical Co., Tokyo, Japan). Sections of 8-μm thickness were stained with hematoxylin and eosin. The frozen slices of brain and liver were reacted with 1 mg/ml 5-bromo-4-chloro-3-indolyl-β-D-galactopyranoside (X-Gal, Wako, Osaka), 50 mM ferrocyanide, 50 mM ferricyanide, 2 mM $MgCl_2$, and 0.1 M sodium acetate (pH 4.5), in 20m M NaCl, for 12 h at 37°C. Serial sections were also immunostained for G_{M1} and G_{A1}. Details of the procedures were described in a previous report (18).

For immunohistochemistry, monoclonal anti-G_{M1} antibody (clone GMB16) and monoclonal anti-G_{A1} antibody (clone AG-1) were purchased from Seikagaku Corporation (Tokyo). Brain tissue sections were permeabilized with 0.25% Triton X-100 in PBS for 15 min at room temperature, blocked with 1% BSA in PBS for 1 h at room temperature, and incubated with the first antibody at 4°C overnight. The anti-G_{M1} had been diluted 1:50 and anti-G_{A1} 1:25 with 0.1% BSA in PBS before use. The sections were washed with 1% BSA in PBS three times for 5 min each at room temperature. Then, they were incubated with FITC-conjugated anti-mouse IgM (1:50 dilution with 0.1% BSA in PBS, washed with PBS 3 times for 5 min each, and mounted on a slide glass (19).

Biochemical Analysis of Mouse Tissues. The left half of the whole brain was used for enzyme assay and lipid analysis. Activities of lysosomal enzymes were assayed by using 4-methylumbelliferyl derivatives (Sigma) as described (20). Protein was determined with the DC Assay Kit (Bio-Rad) or BCA Protein Assay Kit (Pierce).

Total lipids were extracted with chloroform:methanol (2/1, vol/vol) and applied to a chromatography column of DEAE-Sepahadex A-25 (acetate form). Neutral glycosphingolipids were eluted with chloroform:methanol:water (30/60/8, vol/vol/vol), and then gangliosides were eluted with chloroform:methanol:0.8 M sodium acetate (30/60/8, vol/vol/vol) (21). Gangliosides were saponified with 0.5 ml of 0.2 M KOH/methanol, desalted with Sep-Pak C18 reverse-phase cartridge (22) (Waters), and then acetylated with pyridine-acetic anhydride (3:1, vol/vol). Acetylated glycosphingolipids were purified by Sep-Pak Florisil cartridge (Waters) chromatography by using acetone-dichloroethane (1:1, vol/vol) as an elution solvent according to Saito and Hakomori (23). For deacetylation, the acetylated glycosphingolipids were saponified as described in the ganglio-

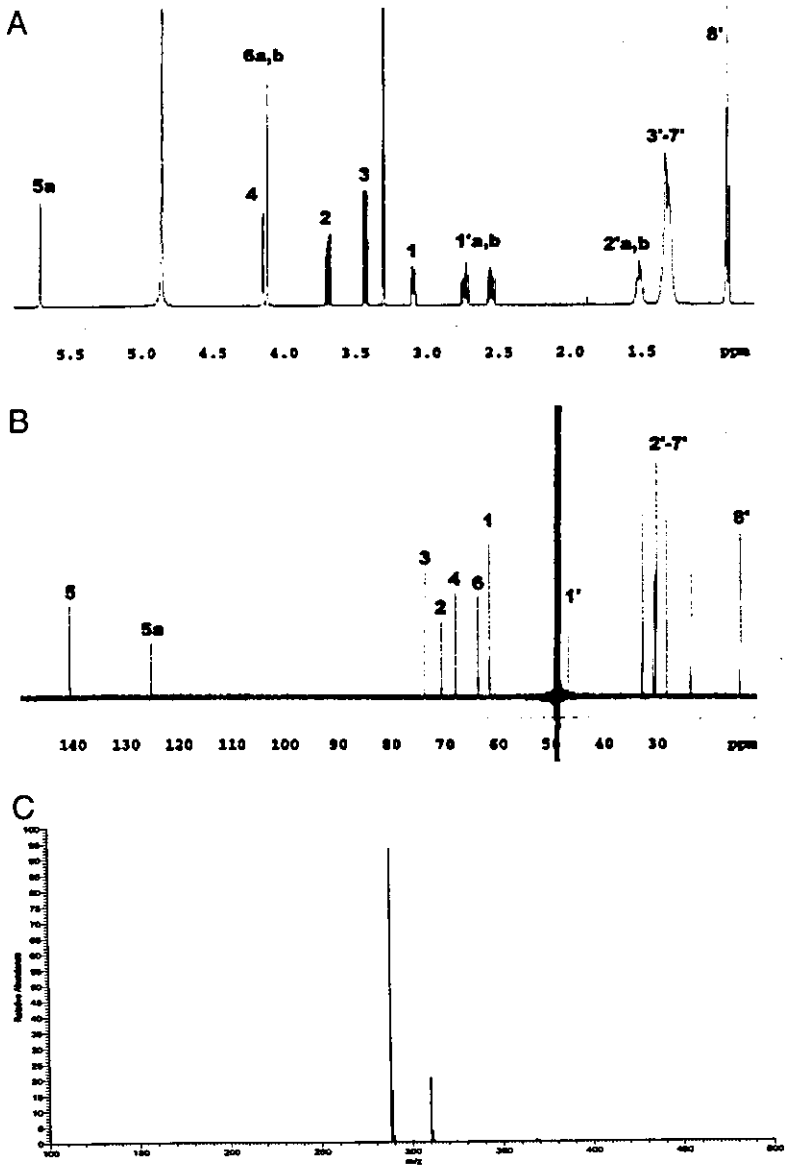

Fig. 2. Spectral data of NOEV. Mass spectrum data of NOEV. (*A*) ^{1}H-NMR. δ 0.900 (t, 3 H, $J_{8'7'}$ = 6.8 Hz, H-8'), 1.290–1.370 (m, 10 H, H-3', 4', 5', 6', and 7'), 1.490–1.540 (m, 2 H, H-2'), 2.555 (ddd, 1 H, J_{gem} = 11.2 Hz, $J_{1'b,2'}$ = 7.4 Hz, H-1'b), 2.739 (ddd, 1 H, J_{gem} = 11.2 Hz, $J_{1'a,2'}$ = 7.4 Hz, H-1'a), 3.101 (dd, 1 H, $J_{1,2}$ = 8.1 Hz, $J_{1,5a}$ = 2.2 Hz, H-1), 3.435 (dd, 1 H, $J_{3,2}$ = 10.0 Hz, $J_{3,4}$ = 4.2 Hz, H-3), 3.696 (dd, 1 H, $J_{2,1}$ = 8.1 Hz, $J_{2,3}$ = 10.0 Hz, H-2), 4.121 (t, 2 H, $J_{6a,6b}$ = 1.7 Hz, H-6a and 6b), 4.154 (d, 1H, $J_{4,3}$ = 4.2 Hz, H-4), 5.718 (d, 1H, $J_{5a,1}$ = 2.2 Hz, H-5a). (*B*) ^{13}C-NMR, δ 14.466 (C-8'), 23.766, 28.480, 30.448, 30.666, 30.983, 33.050 (C-2'~7'), 46.925 (C-1'), 61.848 (C-1), 63.958 (C-6), 68.192 (C-4), 70.862 (C-2), 73.929 (C-3), 125.326 (C-5a), 140.716 (C-5). (*C*) Electrospray ionization mass. $[M + H]^+$, $[M + Na]^+$: *m/z* 288.04, 310.04.

side purification procedure. Individual gangliosides and glycosphingolipids were separated by high performance TLC on a plate precoated with superfine silica gel 60 (Merck, Darmstadt, Germany), with chloroform:methanol:0.2% $CaCl_2$ (60/35/8, vol/vol/vol) for development and visualized with orcinol reagent for qualitative and quantitative analysis (24).

Results

Characterization of NOEV. ^{1}H- and ^{13}C-NMR data of NOEV are shown in Fig. 2 *A* and *B*. The evidence for β linkage was attributed to the doublet signal for H-1 at δ 3.101 ($J_{1,2}$ = 8.1 Hz, $J_{1,5a}$ = 2.2 Hz) (Fig. 2*A*). A positive-ion electrospray ionization (ESI) mass spectrum of NOEV produced peaks at *m/z* 288.04 and 310.04, corresponding respectively to $[M + H]^+$ and $[M + Na]^+$ (Fig. 2*C*). NOEV had R_f 0.33 and 0.24 ($CHCl_3$:MeOH:H_2O, 60:35:8); $[\alpha]_D$ +2.64° (C = 1.03, MeOH) NOEV was found to be stable at room temperature and a strong inhibitor of human β-galactosidase *in vitro*. It is freely soluble in methanol or dimethyl sulfoxide, and it is soluble in water up to 3–5 mM at room temperature. The molecular weight is 287.40. The IC_{50} is 0.2 μM toward human β-galactosidase. This compound did not inhibit galactosyltransferase activity. Accordingly, substrate deprivation did not occur with NOEV.

Effect of NOEV on β-Galactosidase Activity in Cultured Cells. Among the mouse fibroblasts expressing mutant human β-galactosidase R201C and R201H cell strains (14), catalytic activity was markedly increased after exposure to NOEV at 0.2–2 μM in the culture medium for 4 days (Table 1). Lesser augmentation of β-galactosidase activity occurred in fibroblasts with R457Q, W273L, and Y83H mutations. Almost the same or more restorative effect was achieved at 2,500-fold lower concentration than

Table 1. Effect of NOEV on mouse fibroblasts expressing mutant human β-galactosidase

Phenotype	Cell line	Addition: None	DGJ (fold)	NB-DGJ (fold)	NOEV (fold)
Normal	GP8	67.6	112.9 (1.7)	94.5 (1.4)	78.9 (1.2)
Juvenile G_{M1}	R201C	22.9	131.9 (5.8)	113.5 (5.0)	116.3 (5.1)
Adult G_{M1}	R201H	19.1	34.2 (1.8)	52.7 (2.8)	86.0 (4.5)
	R457Q	5.9	31.1 (5.3)	35.6 (6.1)	14.2 (2.4)
Morquio B	W273L	8.1	11.3 (1.4)	11.0 (1.4)	17.7 (2.2)
	Y83H	10.1	17.1 (1.7)	12.4 (1.2)	20.2 (2.0)

Enzyme activity is expressed as nmol/mg of protein per h. Increase after addition is expressed in parentheses as ratio of values with and without inhibitors. G_{M1}, G_{M1}-gangliosidosis; Cell line, cells expressing wild (GP8) or mutant (R201C, R201H, R457Q, W273L, Y83H) β-galactosidase causing various phenotypes of human β-galactosidosis; DGJ, 1-deoxygalactonojirimycin (0.5 mM); NB-DGJ, *N*-butyl-deoxygalactonojirimycin (0.5 mM); NOEV, *N*-octyl-4-epi-β-valienamine (0.2 μM).

that with 1-deoxygalactonojirimycin or *N*-butyl-deoxygalactonojirimycin.

After adding the mixture of gangliosides to the culture medium, intracellular G_{M1} increased remarkably in R201C cells but only slightly in GP8 cells (Fig. 3). Incubation with NOEV significantly reduced G_{M1} storage in R201C cells.

In experiments with human fibroblasts, all of the cells derived from juvenile G_{M1}-gangliosidosis patients and 30% of infantile G_{M1}-gangliosidosis patients expressed an increase of β-galactosidase activity after NOEV treatment (data not shown). Most of them were compound heterozygotes with various mutations, particularly of R201C or R457Q.

KO-Tg Mouse Expressing Human R201C-Mutant β-Galactosidase. The R201C mice, expressing the human R201C-mutant β-galactosidase but lacking the endogenous mouse β-galactosidase, had very low β-galactosidase activity in the brain (≈4% of the wild-type activity). They exhibited an apparently normal clinical course for the first 6 months after birth that was followed by slowly progressive neurological deterioration, such as tremor and gait disturbance during the next 9 months. Death ensued around 15 months of age due to malnutrition and emaciation. Neuropathological examination revealed vacuolated or ballooned neurons, but they were less abundant than those in the KO mouse brain described in our previous reports (17, 18). Intracytoplasmic storage materials were present in pyramidal neurons and brainstem motor neurons, but not in neurons in the other areas of the brain. There was no storage in glial cells.

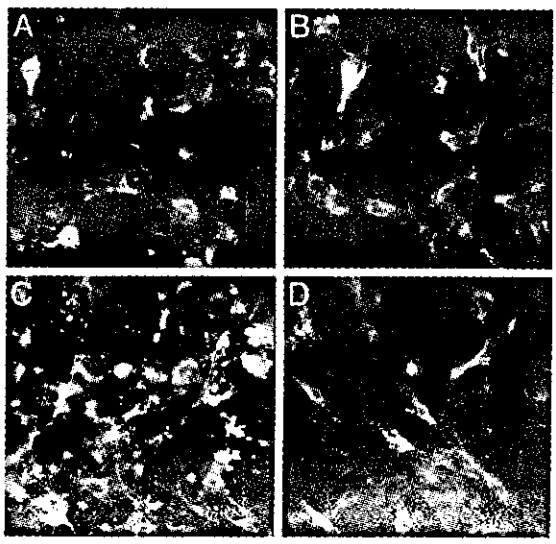

Fig. 3. Effect of NOEV after ganglioside loading on G_{M1} storage in cultured mouse fibroblasts expressing human β-galactosidase gene. The cells expressing mutant (R201C) or wild-type (GP8) human β-galactosidase were loaded with ganglioside mixture, and then cultured with additional 0.2 μM NOEV (4 days). Shown is staining with FITC-labeled cholera toxin B. (*A* and *C*) R201C cells. (*B* and *D*) GP8 cells. (*A* and *B*) After NOEV treatment. (*C* and *D*) Before NOEV treatment. G_{M1} storage was reduced to the control (GP8) level after NOEV treatment. There was no change in GP8 cells.

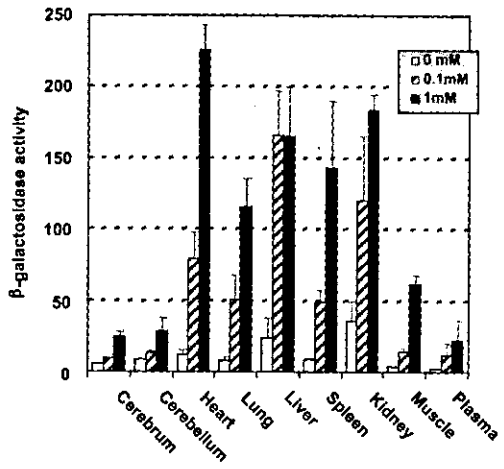

Fig. 4. β-Galactosidase activity in mouse tissues after NOEV treatment. Results are shown for oral administration of NOEV water solution (0.1–1 mM) ad libitum for 1 week to R201C mice (3 months old). β-Galactosidase activity is expressed as nmol/mg of protein per 30 min (mean ± SD; $n = 3$).

Oral Administration of NOEV Restores β-Galactosidase Activity in R201C Mouse Tissues. Aqueous solutions of NOEV (0.1–1 mM) were given ad libitum for 1 week to R201C mice. In this short-term experiment, all of the tissues that were examined showed a remarkable increase of β-galactosidase activity with 1 mM NOEV and a lesser degree with 0.1 mM NOEV (Fig. 4). The increase was relatively high in the heart, lungs, spleen, and muscle as compared with cerebrum and cerebellum. The augmented enzyme activity was sufficient for substrate degradation in these tissues (see below). With 1 mM NOEV, the amount of daily intake was estimated to be 1.4 mg, based on the observation that the daily consumption of water was ≈5 ml per mouse. All of the tissues of mice that received a single daily dose of 0.5 ml of 1 mM NOEV by gavage showed the same increase of β-galactosidase activity that occurred in mice with ad libitum oral daily intake of 5 ml of 0.1 mM NOEV (data not shown).

We used X-Gal staining for evaluation of β-galactosidase expression in individual cells. X-Gal was mainly positive in neurons in the cerebral cortex, thalamus, caudo-putamen, brainstem nuclei, and Purkinje cells, as well as glial cells in cerebral and cerebellar white matter and hepatic cells (Fig. 5). The intensity of staining correlated well with enzyme activity *in vitro*.

Substrate Storage in the Mouse Brain After NOEV Treatment. Immunostaining of the brain tissue revealed a clear decrease of both G_{M1} and G_{A1} in neuronal cells of the fronto-temporal cerebral cortex and brainstem after oral administration of NOEV to the R201C mouse for 1 week (Fig. 6). We did not, however, detect a reduction of G_{M1} or G_{A1} on mass biochemical analysis, presumably because of the short duration of these experiments and localized accumulation of these sphingolipids in neurons in specific regions of the brain.

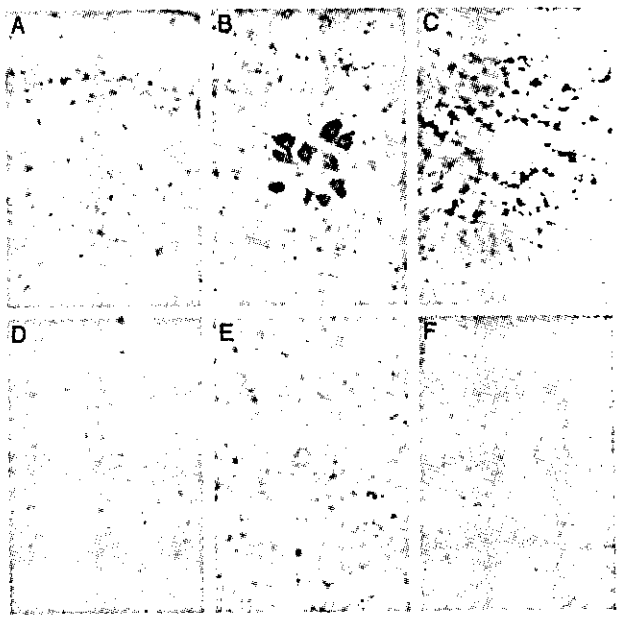

Fig. 5. X-Gal stain of mouse tissues. The R201C mouse, 3 months old, was given orally a water solution of 1 mM NOEV ad libitum for 1 week. The mouse tissues after NOEV treatment are more intensely stained than those without treatment. (*A* and *D*) Fronto-temporal cerebral cortex. (*B* and *E*) Trigeminal nucleus of brainstem. (*C* and *F*) Liver. (*A*, *B*, and *C*) After NOEV treatment. (*D*, *E*, and *F*) Before NOEV treatment. All tissues showed a remarkable increase of X-Gal stain.

Discussion

Low molecular weight compounds for chemical chaperone therapy act as inhibitors at high concentrations *in vitro* and as *in situ* activators at low concentrations. We first demonstrated this apparent paradoxical phenomenon in Fabry disease (4–6) and then in β-galactosidosis (this study) and Gaucher disease (β-glucosidase deficiency) (unpublished data). Intracellular NOEV concentration in the cell and animal experiments in this study must have been much lower than IC_{50} of NOEV *in vitro*. In fact, the concentration of NOEV in the tissue culture medium was approximately the IC_{50} in our cell culture experiments.

In a molecular analysis of G_{M1}-gangliosidosis, Zhang *et al.* (25) reported essentially the same data as ours concerning the mutant enzyme in an infantile patient. The mutation R148S resulted in a major conformational change of the protein molecule with normal catalytic activity. In that case, the mutant protein failed to reach the lysosome and did not express catalytic activity. The report supports the principle of our approach to the molecular rescue of mutant proteins in patients with G_{M1}-gangliosidosis.

Substrate deprivation is another possibility for the treatment of lysosomal storage diseases. *N*-butyl-deoxynojirimycin, an inhibitor of ceramideglucosyltransferase, produced clinical and morphological effects in the Tay-Sachs mouse (26), Sandhoff mouse (27), and Fabry mouse (28), and in patients with Gaucher disease (29). For chemical chaperone therapy, only a low level of the material is needed for restoration of the catalytic activity of mutant enzymes compared with that for inhibition of biosynthetic reactions. It is hoped that the administration of such low levels of useful inhibitors would occur without clinical problems.

Chemical chaperone therapy has two major advantages over enzyme replacement therapy, oral administration and accessibility to the brain. NOEV administration in this study was for a short-term, and we did not anticipate a decrease in overall substrate storage in the brain of experimental animals in the late-onset type disease. The R201C mutation causes a mild clinical phenotype of G_{M1}-gangliosidosis, and substrate storage is not full-blown in the early stage of life either in mice or humans. Intracytoplasmic ballooning was observed only in pyramidal cells and brainstem motor neurons in the R201C mouse brain. Because of the brief duration of the investigation and potential limitation of high glycosphingolipid turnover to neuronal cells in the fronto-temporal cerebral cortex and brainstem, we did not see a reduction of G_{M1} or G_{A1} on mass biochemical

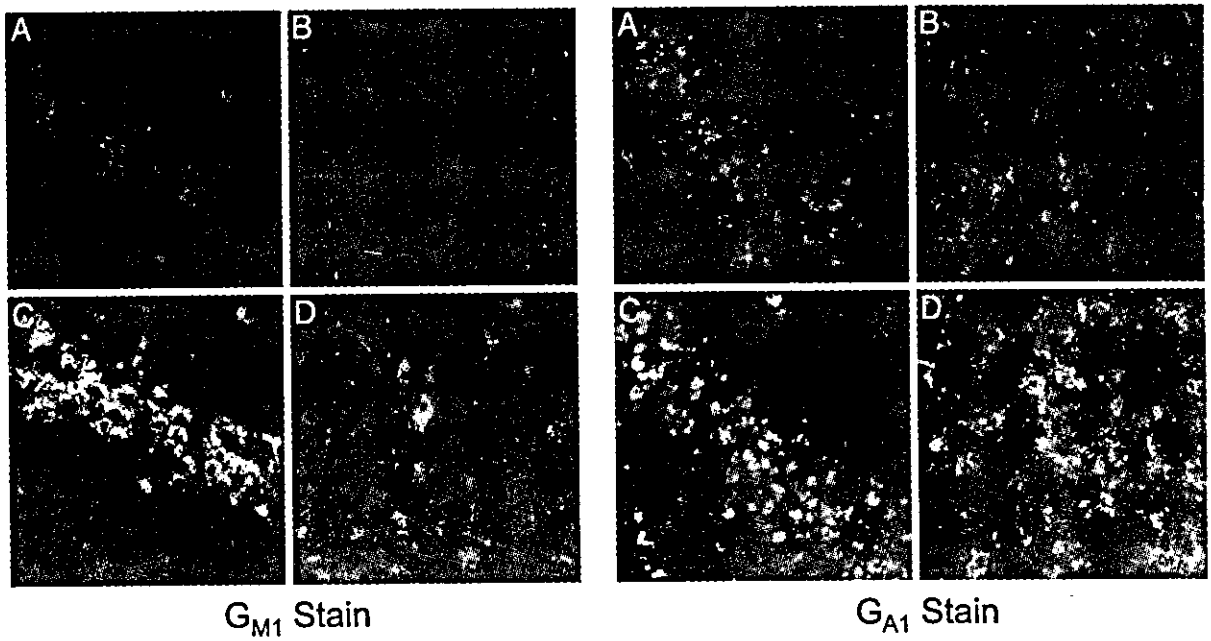

Fig. 6. Immunostaining of G_{M1} and G_{A1} in the mouse brain. The R201C mouse, 3 months old, was given orally a water solution of 1 mM NOEV ad libitum for 1 week, and the fronto-temporal cortex and brainstem were stained as described in *Materials and Methods*. (*A* and *C*) Fronto-temporal cerebral cortex. (*B* and *D*) Trigeminal nucleus of brainstem. (*A* and *B*) After NOEV treatment. (*C* and *D*) Before NOEV treatment. A remarkable decrease of both G_{M1} and G_{A1} is observed in the brain after the NOEV treatment.

analysis. More time may be needed to demonstrate a mass substrate reduction in the brain of the model mouse that represents juvenile G_{M1}-gangliosidosis with a protracted clinical course.

We also need long-term experiments to establish an optimal dose for prevention or reduction of substrate storage in these mice. Possible adverse or toxic effects should be carefully evaluated before starting human clinical experiments. We are aware that this molecular approach is not justified for all patients with a single lysosomal enzyme deficiency disorder. Biosynthesis of a catalytically active enzyme is prerequisite in chemical chaperone therapy. Our initial survey indicates that at least 30% of β-galactosidosis (mainly G_{M1}-gangliosidosis) patients express unstable but catalytically active protein and respond to NOEV treatment in cultured fibroblasts. Patients of this type may be reasonable candidates for chemical chaperone therapy. This strategy is in principle applicable to all lysosomal storage diseases if specific compounds can be found for each enzyme that is involved. Special drug design technology may be needed to screen appropriate inhibitors. Bioinformatics analysis may reveal a new aspect of molecular pathology in lysosomal storage diseases (30, 31) and be a useful adjunct for the development of effective chemical chaperone therapy.

We thank the following investigators for supplying human fibroblasts in this study: Nils U. Bosshard (University Children's Hospital, Zurich), Koji Inui (Osaka University, Osaka), Jana Ledvinova (Charles University, Prague), Gert Matthijs (Universitaire Ziekenhuizen, Leuven), Toshihiro Oura (Tohoku University, Sendai), Alan Percy (The Children's Hospital of Alabama), Konrad Sandhoff and Gerhild van Echten-Deckert (Kekule-Institut für Organische Chemie und Biochemie, Bonn), George H. Thomas (Kennedy Krieger Institute, Baltimore), David A. Wenger (Thomas Jefferson University, Philadelphia), and Marie-Therese Zabot (Hôpital Debrousse, Lyon). This research was supported by Ministry of Education, Culture, Science, Sports, and Technology of Japan Grants 13680918 and 14207106, and Ministry of Health, Labour, and Welfare of Japan Grant 14221201.

1. Suzuki, Y., Oshima, A. & Nanba, E. (2001) in *The Metabolic and Molecular Bases of Inherited Disease*, eds. Scriver, C. R., Beaudet, A. L., Sly, W. S., Valle, D., Childs, B. & Vogelstein, B. (McGraw-Hill, New York), 8th Ed., pp. 3775–3809.
2. O'Brien, J. S., Storb, R., Raff, R. F., Harding, J., Appelbaum, F., Morimoto, S., Kishimoto, Y., Graham, T., Ahern Rindell, A. & O'Brien, S. L. (1990) *Clin. Genet.* **38,** 274–280.
3. Tylki-Szymanska, A., Maciejko, D., Kidawa, M., Jablonska-Budaj, U. & Czartoryska, B. (1985) *J. Inherit. Metab. Dis.* **8,** 101–104.
4. Okumiya, T., Ishii, S., Takenaka, T., Kase, R., Kamei, S., Sakuraba, H. & Suzuki, Y. (1995) *Biochem. Biophys. Res. Commun.* **214,** 1219–1224.
5. Fan, J. Q., Ishii, S., Asano, N. & Suzuki, Y. (1999) *Nat. Med.* **5,** 112–115.
6. Ishii, S., Kase, R., Sakuraba, H., Taya, C., Yonekawa, H., Okumiya, T., Matsuda, Y., Mannen, K., Takeshita, M. & Suzuki, Y. (1998) *Glycoconj. J.* **15,** 591–594.
7. Okumiya, T., Ishii, S., Kase, R., Kamei, S., Sakuraba, H. & Suzuki, Y. (1995) *Hum. Genet.* **95,** 557–561.
8. Ishii, S., Kase, R., Okumiya, T., Sakuraba, H. & Suzuki, Y. (1996) *Biochem. Biophys. Res. Commun.* **220,** 812–815.
9. Ogawa, S., Tsunoda, H. & Inokuchi, J.-i. (1994) *J. Chem. Soc. Chem. Commun.* 1317–1318.
10. Tsunoda, H., Inokuchi, J.-i., Yamagishi, K. & Ogawa, S. (1995) *Liebigs Ann.* 279–284.
11. Ogawa, S., Ashiura, M., Uchida, C., Watanabe, S., Yamazaki, C., Yamagishi, K. & Inokuchi, J.-i. (1996) *Bioorg. Med. Chem. Lett.* **6,** 929–932.
12. Ogawa, S., Kobayashi, Y., Kabayama, K., Jimbo, M. & Inokuchi, J.-i. (1998) *Bioorg. Med. Chem.* **6,** 1955–1962.
13. Ogawa, S., Matsunaga, Y. K. & Suzuki, Y. (2002) *Bioorg. Med. Chem.* **10,** 1967–1972.
14. Tominaga, L., Ogawa, Y., Taniguchi, M., Ohno, K., Matuda, J., Oshima, A., Suzuki, Y. & Nanba, E. (2001) *Brain Dev.* **23,** 284–287.
15. Sugimoto, Y., Ninomiya, H., Ohsaki, Y., Higaki, K., Davies, J. P., Ioannou, Y. A. & Ohno, K. (2001) *Proc. Natl. Acad. Sci. USA* **98,** 12391–12396.
16. Zhang, H., Nanba, E., Yamamoto, T., Ninomiya, H., Ohno, K., Mizuguchi, M. & Takeshita, K. (1999) *J. Hum. Genet.* **44,** 391–396.
17. Matsuda, J., Suzuki, O., Oshima, A., Ogura, A., Noguchi, Y., Yamamoto, Y., Asano, T., Takimoto, K., Sukegawa, K., Suzuki, Y., *et al.* (1997) *Glycoconj. J.* **14,** 729–736.
18. Itoh, M., Matsuda, J., Suzuki, O., Ogura, A., Oshima, A., Tai, T., Suzuki, Y. & Takashima, S. (2001) *Brain Dev.* **23,** 379–384.
19. Taniguchi M., Shinoda Y., Ninomiya H., Vanier M. T. & Ohno K. (2001) *Brain Dev.* **23,** 414–421.
20. Sakuraba, H., Aoyagi, T. & Suzuki, Y. (1982) *Clin. Chim. Acta* **125,** 275–282.
21. Yu, R. K. & Ledeen, R. W. (1972) *J. Lipid Res.* **13,** 680–686.
22. Williams, M. A. & McCluer, R. H. (1980) *J. Neurochem.* **35,** 266–269.
23. Saito, T. & Hakomori, S. I. (1971) *J. Lipid Res.* **12,** 257–259.
24. Sewell, A. C. (1979) *Clin. Chim. Acta* **92,** 411–414.
25. Zhang, S., Bagshaw, R., Hilson, W., Oho, Y., Hinek, A., Clarke, J. T. & Callahan, J. W. (2000) *Biochem. J.* **348,** 621–632.
26. Platt, F. M., Neises, G. R., Reinkensmeier, G., Townsend, M. J., Perry, V. H., Proia, R. L., Winchester, B., Dwek, R. A. & Butters, T. D. (1997) *Science* **276,** 428–431.
27. Jeyakumar, M., Butters, T. D., Cortina-Borja, M., Hunnam, V., Proia, R. L., Rerry, V. H., Dwek, R. A. & Platt, F. M. (1999) *Proc. Natl. Acad. Sci. USA* **96,** 6388–6393.
28. Platt, F. M., Jeyakumar, M., Andersson, U., Heare, T., Dwek, R. A. & Butters, T. D. (2003) *Philos. Trans. R. Soc. London B. Biol. Sci.* **358,** 947–954.
29. Cox, T., Lachmann, R., Hollak, C., Aerts, J., van Weely, S., Hrebicek, M., Platt, F., Butters, T., Dwek, R., Moyses, C., *et al.* (2000) *Lancet* **355,** 1481–1485.
30. Durand, P., Fabrega, S., Henrissat, B., Mornon, J.-P. & Lehn, P. (2000) *Hum. Mol. Genet.* **9,** 967–977.
31. Fabrega, S., Durand, P., Codogno, P., Bauvy, C., Delomenie, C., Henrissat, B., Martin, B. M., McKinney, C., Ginns, E. I., Mornon, J. P., *et al.* (2000) *Glycobiology* **10,** 1217–1224.

Gene Therapy (2003) 10, 1487–1493

www.nature.com/gt

RESEARCH ARTICLE

Attenuation of ganglioside GM1 accumulation in the brain of GM1 gangliosidosis mice by neonatal intravenous gene transfer

N Takaura[1], T Yagi[2], M Maeda[2], E Nanba[3], A Oshima[4], Y Suzuki[5], T Yamano[1] and A Tanaka[1]

[1]*Department of Pediatrics, Osaka City University Graduate School of Medicine, Osaka, Japan;* [2]*Department of Neurobiology and Anatomy, Osaka City University Graduate School of Medicine, Osaka, Japan;* [3]*Gene Research Center, Tottori University, Yonago, Japan;* [4]*Department of Pediatrics, Takagi Hospital, Saitama, Japan; and* [5]*Pediatrics, Clinical Research Center, Nasu Institute for Developmental Disabilities, International University of Health and Welfare, Ohtawara, Japan*

A single intravenous injection with 4 × 10⁷ PFU of recombinant adenovirus encoding mouse β-galactosidase cDNA to newborn mice provided widespread increases of β-galactosidase activity, and attenuated the development of the disease including the brain at least for 60 days. The β-galactosidase activity showed 2–4 times as high a normal activity in the liver and lung, and 50 times in the heart. In the brain, while the activity was only 10–20% of normal, the efficacy of the treatment was distinct. At the 30th day after the injection, significant attenuation of ganglioside GM1 accumulation in the cerebrum was shown in three out of seven mice. At the 60th day after the injection, the amount of ganglioside GM1 was above the normal range in all treated mice, which was speculated to be the result of reaccumulation. However, the values were still definitely lower in most of the treated mice than those in untreated mice. In the histopathological study, X-gal-positive cells, which showed the expression of exogenous β-galactosidase gene, were observed in the brain. It is noteworthy that neonatal administration via blood vessels provided access to the central nervous system because of the incompletely formed blood–brain barrier.

Gene Therapy (2003) **10**, 1487–1493. doi:10.1038/sj.gt.3302033

Keywords: *GM1 gangliosidosis; neonatal gene transfer; intravenous administration; brain gene therapy*

Introduction

A number of therapeutic experiments using the murine models have been performed for various lysosomal enzyme deficiencies, such as mucopolysaccharidosis VII (MPS VII) mouse.[1,2] For the treatment of lysosomal storage disease (LSD), the enzyme does not necessarily need to be produced within the affected cells, but can be taken up from the extracellular milieu via binding to mannose-6-phosphate receptors on the cell surface in many of the lysosomal enzymes.[3] Thus, the deficient enzyme can be supplied with the administered enzyme protein or the secreted enzyme from the transplanted normal cells or genetically reconstructed cells secreting the enzyme protein. This ability of cells to internalize lysosomal enzymes and direct them to the lysosomal compartment forms the biochemical basis of the potential for the therapeutic strategies for LSD.

Enzyme replacement therapy (ERT),[4,5] bone marrow transplantation (BMT),[1,6,7] and gene transfer[2,8] have been studied in animals and in humans with LSDs. ERT is clinically available for Gaucher disease[9] and Fabry disease[10] as medicine in many countries, and they are very effective. ERTs for MPS I, II, and glycogen storage disease type II are ongoing to clinical uses. However, the effects of ERT are transient, requiring repeated administrations of the enzyme protein throughout life to maintain activity and to prevent the disease. Moreover, no effect is shown on the brain because of the blood–brain barrier. BMT is effective on the somatic involvement of LSDs.[6,11] However, the uses of BMT are limited for the lack of appropriate donors, or morbidity associated with allogeneic transplantation. Moreover, bone and the brain are the exceptions to the effects of BMT. Gene transfer using virus vectors via blood vessels is also effective on various organs.[2] The transduced cells would make the enzyme protein from the transferred gene to be reconstituted, and the enzyme protein could be secreted from the cells and be delivered to uninfected cells locally or distantly. However, only direct injections of the gene into the brain or into the ventricle have been shown to be effective on the central nervous system.[12–14] The blood–brain barrier blocks the enzyme protein-mediated correction or the gene transfer into the brain in any of these approaches. According to the previous literatures, neonatal treatments of ERT or BMT provide a more complete correction in many organs, even in the brain.[15–17] It has been reported that neonatal gene transfer in MPS VII mouse provided sufficient effects on most tissues including the brain.[18,19]

Correspondence: Dr A Tanaka, Department of Pediatrics, Osaka City University Graduate School of Medicine, 1-4-3 Asahi-machi, Abeno-ku, Osaka 545-8585, Japan
Received 22 November 2002; accepted 18 February 2003

We focused our studies on the treatment of the brain for GM1 gangliosidosis. GM1 gangliosidosis is a member of LSDs, which shows a progressive neurological disease in humans caused by the genetic defect of lysosomal acid β-galactosidase that hydrolyses the terminal β-galactosidic residue of ganglioside GM1 and other glycoconjugates.[20] The defects of the β-galactosidase activity result in an accumulation of ganglioside GM1 in various organs especially in the brain, which causes the progressive neurodegeneration. Since the gene transfer by intracranial injection is an invasive therapy for the patients, we carried out our study of treating the brain by intravenous gene transfer for the murine model of GM1 gangliosidosis. As it is speculated that protective protein/cathepsin A is needed for β-galactosidase stabilization, β-galactosidase may not be amenable to treatment by the overexpression from the exogenous gene. However, we could show that intravenous gene transfer into the brain was reliable in neonatal period and a small amount of β-galactosidase activity would be sufficient for the brain to prevent the disease progression. It is obvious that the success of the brain therapy in GM1 gangliosidosis mouse provides a promising tool for the brain treatment of LSDs in general.

Results

Enzyme activity

β-Galactosidase activity in HeLa cells and in the culture medium infected at multiplicity of infection (MOI) 40 by the recombinant adenovirus vector carrying mouse β-galactosidase cDNA were 3–5 times and 40–50 times higher than in the cells and in the medium with mock infection, respectively (data not shown).

β-Galactosidase activity in each organ obtained at the 30th and 60th days after the injection was shown in Table 1. In treated mice, the β-galactosidase activity of the liver and the heart increased definitely in every sample, while the activity of other organs did not increase in a few samples. The maximum increase of the activity was remarkable in the liver, lung, and the heart. The activities at the 60th day were lower than those at the 30th day in most of the samples. Very large deviation values in the increased activities were seen in every organ. Figure 1 shows the activities in each organ of each mouse at the 30th day. The levels of the activity in each organ showed a similar feature among the mice, but the ratio of the increased activity in each organ was very different and did not show a parallel view among the mice. A slight increase of β-galactosidase activity in the brain was detected, and the increases in some mice were significant as shown in Table 2.

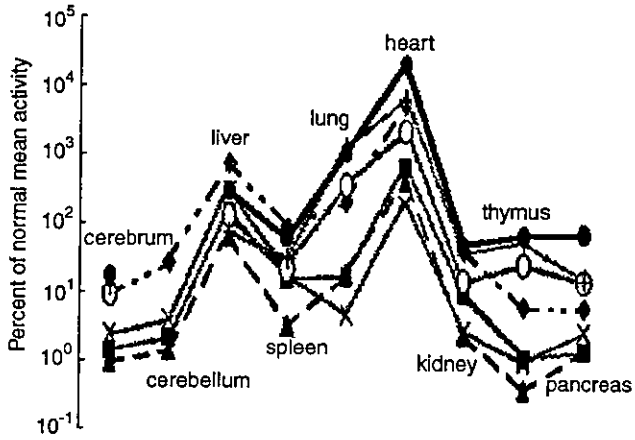

Figure 1 β-Galactosidase activity in tissue homogenates at the 30th day after treatment (n=7). The values of each organ were connected with lines individually. The activities in the organs did not show parallel increase.

Table 1 β-Galactosidase activity in each organ

Organ	*Treated*	*Untreated*	*Normal*
30th day	*n*=7	*n*=6	*n*=5
Cerebrum	0.62–11.6	2.45±1.46	67.1±11.1
Cerebellum	0.60–11.5	ND	45.3±6.5
Liver	35.6–415	1.17±0.57	48.4±22.2
Spleen	4.78–129	4.27±0.66	145±27
Lung	3.65–965	4.45±1.81	77.7±14.8
Heart	57.9–1940	2.00±1.12	28.6±2.1
Kidney	2.72–55.8	16.6±7.87	101±16
Thymus	0.332–58.8	2.19±0.71	93.3±25.6
Pancreas	0.785–40.3	1.20±0.34	52.7±12.9
60th day	*n*=10	*n*=9	*n*=4
Cerebrum	1.83–16.1	2.53±0.39	42.6±16.1
Cerebellum	ND	ND	ND
Liver	22.6–201	1.33±0.41	89.5±12.6
Spleen	22.5–94.5	10.3±4.2	221±65
Lung	28.5–351	4.76±2.38	75.0±9.2
Heart	112–1510	1.39±0.28	21.2±3.2
Kidney	8.59–73.5	12.4±4.2	111±8
Thymus	3.04–141	3.22±0.58	112±28
Pancreas	0.482–17.4	1.03±0.32	78.5±33.0

The values were shown by the range of activity in the treated mice and by mean value±1SD of activity in untreated mice and in normal mice of each organ (unit: nmol/mg/h). ND, not determined.

Table 2 β-Galactosidase activity and the amount of ganglioside GM1 in the brain

	β-Galactosidase activity (nmol/mg/h)	*Ganglioside GM1 (μmol/g)*[a]	
Mouse no.	*Cerebrum*	*Cerebrum*	*Cerebellum*
30th day			
Treated 1	6.15[b]	1.03[c]	0.81
2	0.939	1.57	1.18
3	0.615	2.01	1.68
4	1.57	2.04	0.68
5	11.6[b]	0.49[c]	0.72
6	6.16[b]	0.48[c]	0.29[c]
7	8.46[b]	0.36[c]	0.28[c]
Untreated (n=8)[d]	3.38±2.14	1.68±0.23	1.24±0.58
Normal (n=7)[d]	67.4±19.1	0.17±0.08	0.26±0.23
60th day			
Treated 1	2.62	2.16[c]	2.35
2	4.36[b]	2.33	0.80[c]
3	16.1[b]	0.99[c]	0.35[c]
4	2.47	1.79[c]	3.02
5	2.71	4.01	1.63
6	1.83	4.56	1.61
7	8.59[b]	2.06[c]	1.07[c]
8	4.63[b]	1.97[c]	1.63
9	8.30[b]	1.64[c]	1.54
10	6.22[b]	1.88[c]	1.22[c]
Untreated (n=12)[d]	2.65±0.45	3.22±1.00	2.19±0.94
Normal (n=6)[d]	45.8±12.2	0.32±0.07	0.20±0.04

[a]Shown in μmol/g wet weight of tissue.
[b]Higher activity of β-galactosidase than mean value 1SD of untreated group.
[c]Lower amount of ganglioside GM1 than mean value 1SD of untreated group.
[d]Shown in mean±1SD.

Ganglioside GM1 analysis by thin-layer chromatography (TLC)

Figure 2 shows the thin-layer chromatogram of the brain extracts. The accumulation of ganglioside GM1 in the brain was almost corrected in some of the treated mice at the 30th day after the injection. The accumulation of ganglioside GM1 in the liver was corrected in every treated mouse (data not shown).

Table 2 shows the β-galactosidase activity and the amount of ganglioside GM1 of brain in each treated mouse, and the mean±1SD values in untreated knock-out mice and normal control mice. At the 30th day, four (mouse nos. 1, 5, 6, and 7) out of seven mice showed higher activity of β-galactosidase and a significant decrease of ganglioside GM1 accumulation in the cerebrum. Three mice of the remaining (nos. 2, 3, and 4) did not show any increase of the β-galactosidase activity or attenuation of the disease in the brain. At the 60th day, five (mouse nos. 3, 7, 8, 9, and 10) out of 10 mice showed higher activity of β-galactosidase corresponding to the decrease of ganglioside GM1 in cerebrum. An excellent efficacy was shown in mouse no. 3, which still had a significant higher activity of β-galactosidase and a lower amount of ganglioside GM1 accumulation. The amounts of ganglioside GM1 were significantly lower in most of the treated mice than those in the untreated mice, but were definitely higher than those in normal mice.

In the liver, β-galactosidase activity showed 73–857% of the mean value of normal activity at the 30th day, which resulted in the prevention of ganglioside GM1 accumulation almost completely (data not shown). At the 60th day, β-galactosidase activity in the liver still showed 25–225% of the normal activity, and the continuous prevention of ganglioside GM1 accumulation was observed (data not shown).

Histopathological studies

β-Galactosidase-positive cells by X-gal staining were detected in various organs (data not shown) including the brain. X-gal stainings of the brain and the liver are shown in Figures 3 and 5. Figures 4a and b show anti-GM1 ganglioside staining of the brain in treated and untreated mouse, respectively. The amount of immunoreactive materials was definitely less in the treated mouse than in the untreated mouse, indicating attenuation of ganglioside GM1 accumulation by the neonatal gene transfer. The percentages of the infected cells counted in the specimen with X-gal staining were 0–1% in the brain and 5–10% in the liver.

Discussion

A single intravenous injection of recombinant adenovirus encoding mouse β-galactosidase cDNA for newborn mice provided widespread increases of β-galactosidase activity and attenuated the development of the disease including the brain at least for 60 days.

It is noteworthy that neonatal administration via blood vessels provided access to the brain, and it is a noninvasive method. Although the activity in the treated brain was not remarkable, the accumulation of

ganglioside GM1 was attenuated definitely in three out of seven mice at the 30th day (Table 2, mouse nos. 5, 6 and 7). The efficacy was clearly confirmed by biochemical analysis of TLC (Figure 2) and histochemical analysis of immunostaining (Figure 4a and b). It is consistent with the clinical fact that a very slight residual catalytic activity in the patients attenuates the symptoms, and results in a mild phenotype.[20] At the 60th day after the treatment, the amount of ganglioside GM1 was above the normal range in all treated mice, which was speculated to be the result of reaccumulation. However, the values were still definitely lower in most of the treated mice than those in untreated mice (Table 2). The continuous activity of β-galactosidase about 15–20 nmol/mg/h (20% of normal activity) in the brain would be sufficient to prevent the disease.

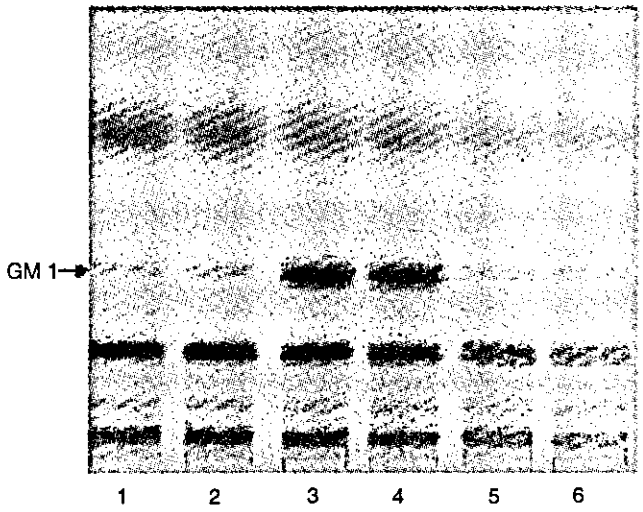

Figure 2 Thin-layer chromatography of lipids in the brain tissue extracts. Lanes 1 and 2, treated mouse; 3 and 4, untreated mouse; 5 and 6, normal mouse. Each sample was applied on two separate lanes to confirm the measurement. Each lipid extract from 4 mg in wet weight of cerebrum was applied on TLC plate. The separated lipids were visualized by resorcinol spray. The arrow indicates the band of ganglioside GM1. The pattern of TLC and the amount of ganglioside GM1 in the treated mice were similar to those of normal mouse. Each one of the two lanes from the same samples showed completely the same pattern of chromatogram and the values obtained by densitometric qantification were almost equal.

A small number of cells stained with X-gal, which means the expression of β-galactosidase activity in the cells, were found in the cerebrum of the mice with good efficacy at the 30th day after treatment (Figure 3). These cells were away from the blood vessels and appeared to be neuronal cells from their shape, which leads to the speculation that adenovirus particles got into the brain through the blood–brain barrier via blood vessels and infected the cells.

The efficacy on the attenuation of ganglioside GM1 accumulation was consistent with the increase in β-galactosidase activity. Good efficacy was observed in the liver of every treated mouse, while the efficacy was varied and limited in the brain. The difference in the efficacy on the brain among the treated mice might be caused by the different efficiency of adenovirus infection, which resulted from the different permeability of the blood–brain barrier. Although the adenovirus injections were carried out at 24–48 h after birth, the maturation of

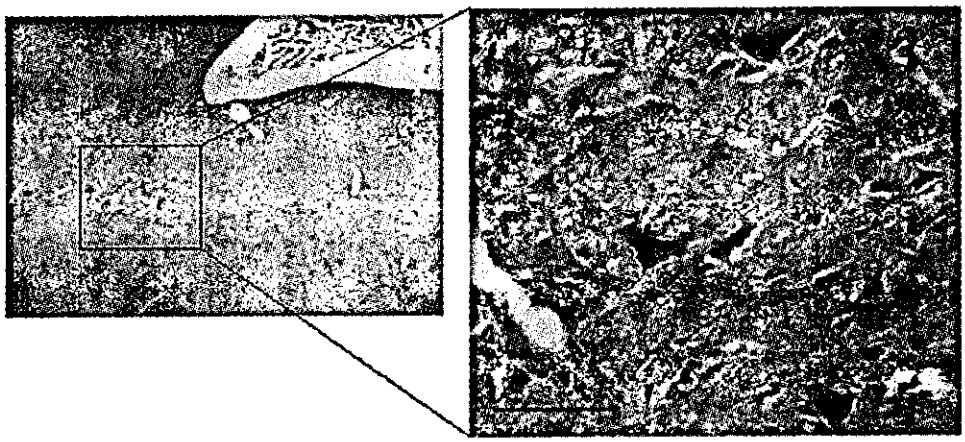

Figure 3 X-gal staining of the cerebrum in a treated mouse at the 30th day. Several positive-staining cells showing strong blue color were found. They were speculated to be neuronal cells from their shape. Scale bar=50 μm.

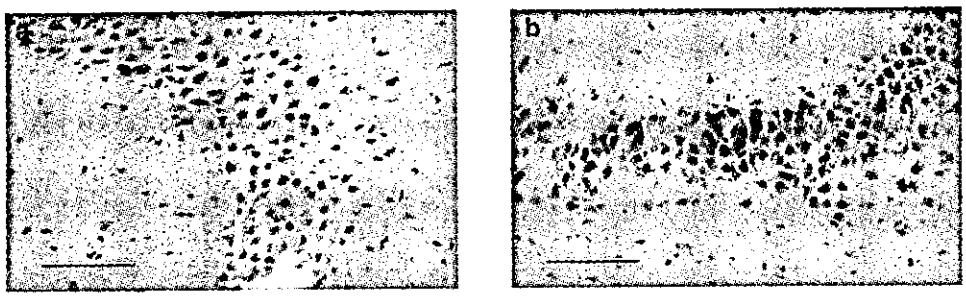

Figure 4 Antiganglioside GM1 antibody immunostaining of the cerebrum in treated (a), and in untreated (b) knockout mouse at the 30th day. The positive cells were definitely deceased in the brain of treated mouse. Scale bars=100 μm.

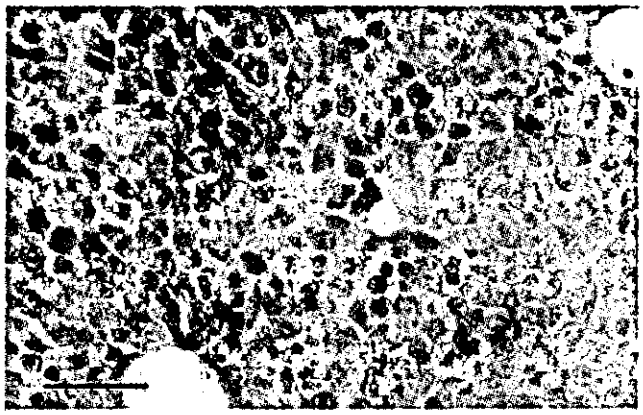

Figure 5 X-gal staining of the liver in a treated mouse at the 30th day. Many positive-staining cells were spread diffusely in the whole organ. Scale bar=100 μm.

blood–brain barrier would be definitely different between at 24 h and at 48 h because the brain of the newborn mouse develops very rapidly.

The activities of β-galactosidase were very much increased in the liver, lung, and the heart (Table 1), where the high vascularity and abundant blood flow may give predominance of adenovirus infection. Moreover, large deviations of activity among the treated mice would suggest that the activity resulted from the infectious efficiency. The primary source of β-galactosidase activity is speculated to be direct infection by adenovirus, not cross-correction by secreted enzyme. This hypothesis is supported by the fact that the activities in each organ in treated mice were not parallel among the organs (Figure 1). In other words, the mouse having the highest activity in the liver did not necessarily have the highest activity in the brain, and *vice versa*.

Although the direct infection of tissues by adenovirus vector seems to be the primary source of β-galactosidase activity, interorgan and intraorgan cross-correction by circulating enzyme must also be a factor. The interorgan cross-correction might play a major role in the early stage of infection when high levels of serum activity are present. Since the blood–brain barrier is not fully intact until 10–14 days of life in rodents,[21] it would be possible for the proteins to enter from blood flow into the brain, as well as for the virus particles. The evidence of intraorgan cross-corrections was shown both in the brain and in the liver of this study. The remarkable attenuation of ganglioside GM1 accumulation in the brain and the liver was shown in some treated mice by biochemical analysis, while only a small number of cells (less than 1 and 10% of the cells in the brain and in the liver, respectively) were positive with X-gal staining (Figures 3 and 5). Since the infected cells are the only source of the β-galactosidase activity in the brain after the closure of the blood–brain barrier, the vector expressing the enzyme activity constitutively is needed for the successful prevention of the disease. As the maturation of blood–brain barrier in the human, which is completed by birth, is definitely different from that in the mouse, intrauterine treatment may be needed for human patients. However, the treatment before the massive accumulation occurs is important definitely, and it would be possible that the low level but persisting activity of the enzyme could prevent the further accumulation and the disease development throughout life.

Materials and methods

GM1-gangliosidosis mouse model (β-galactosidase-deficient mouse)

Mouse model of GM1 gangliosidosis was generated by targeting of β-galactosidase gene in ES cells as previously described.[22,23] Newborn mice were obtained by mating the heterozygous female mice with the homozygous male mice. Identification of newborn mutants was accomplished by quantitative analysis of β-galactosidase activity in the tail tip homogenates on the day of birth. Age-matched wild-type mice of C57BL/6 strain were used as the control.

All surgical and care procedures were carried out according to the Guidelines for Use and Care of Experimental Animals approved by the Animal Committee of Osaka City University School of Medicine.

Construction of adenovirus vector with β-galactosidase cDNA

AdEasy system,[24] the system for constructing adenovirus vector, was kindly provided by Dr. Vogestein at Johns Hopkins Oncology Center. Mouse β-galactosidase cDNA was cloned and constructed as previously reported.[25] Construction of adenovirus vector carrying mouse β-galactosidase cDNA was performed by the protocol described at http://www.coloncancer.org/adeasy/protocol.htm. Mouse β-galactosidase cDNA was cloned into the shuttle vector pAdTrackCMV having GFP gene as a reporter, linearized by digesting with *Pme*I, and cotransformed by electroporation with an adenoviral backbone plasmid pAdEasy-1 into *E. coli* BJ5183 cells. Recombinants were selected for kanamycin resistance, and linearized by digesting with *Pac*I, then transfected by Lipofectamine (GIBCO BRL, Rockville, MD, USA) into the 293 adenovirus packaging cells. Recombinant adenoviruses were generated within 7–12 days. The recombinant virus solution was obtained by removing the host cells by sonication and centrifugation. The virus was amplified by repeating the infection with the viral supernatant. The concentration of viral solution was achieved finally at 3.93×10^9 PFU/ml.

To confirm the virus activity, infection to HeLa cells was performed at an MOI of 40. The infection and the protein formation by the recombinant virus were determined by GFP fluorescence on microscope and the analysis of β-galactosidase activity in the cell homogenate and in the culture medium.

Administration of adenovirus vector and the preparation of tissues

Each mouse received a single intravenous injection of 100 μl of viral suspension with 4×10^7 PFU via the superficial temporal vein from 24 to 48 h after birth. Mice were examined on the 30th and the 60th days after birth. One hemisphere of the brain was used for biochemical analyses, and the other was used for histological examinations in each mouse.

For the biochemical analysis, mice were anesthetized with diethylether and the blood was washed out with

normal saline by perfusing through the heart, and each organ was wrapped with Parafilm and kept at −80°C until use. For the histological studies, the organs were fixed by perfusing through the heart with 4% paraformaldehyde in 0.1 M phosphate buffer pH 7.4 (PB) for 20 min, after washing out the blood with normal saline. The organs were placed in the same fixing mixture overnight for paraffin sections. For the use of frozen sections, the tissues were placed in 0.1 M phosphate buffer pH 7.4 containing 30% sucrose, then frozen in liquid nitrogen.

β-Galactosidase assay

β-Galactosidase activity was analyzed in the tissue homogenate with the artificial substrate of 2 mM 4-methylumbelliferyl β-galactoside at pH 4.0 in 0.1 M sodium citrate-phosphate buffer according to the method described by Suzuki.[26] The protein was analyzed by using Bio-Rad protein assay system (Bio-Rad Laboratories, Hercules, CA, USA) of Bradford.[27]

Ganglioside analysis

Lipid extraction, ganglioside isolation, and lipid quantification were performed as described by Fujita *et al*[28] and Hahn *et al*[29]. Total lipids were extracted from tissue homogenate in chloroform–methanol (1:2, v/v). Neutral and acidic fractions were separated by reverse-phase column of Varian Bond Elute C-18 (GL Sciences Inc, Tokyo, Japan). The column was preconditioned with chloroform–methanol (1:2, v/v) and 99.5% methanol. The lipids extracted from 100 to 200 mg in wet weight of each tissue were applied onto the column, and the column was washed with methanol–0.9% saline (1:1, v/v). Ganglioside/acidic lipids were eluted with methanol–water (12:1, v/v) and collected for the study. The content of sialic acid in the ganglioside/acidic lipid fraction was analyzed by the colorimetric assay by the resorcinol method[30] with *N*-acetylneuraminic acid as the standard. Lipids were separated by TLC with high-performance thin-layer plates (Merck High-Performance TLC 60; Merck KGaA, Darmstadt, Germany) and developed in the solvent of chloroform–methanol–0.2% $CaCl_2$ (55:45:10; v/v/v). Gangliosides were visualized by resorcinol spray and heating. Each sample was applied in two lanes and repeated twice to show the reliability of the TLC technique. Densitometric quantification of gangliosides was performed using Kodak Digital Science™ EDAS 120 system with 1D Image Analysis software (Eastman Kodak Company, NY, USA). The analysis was carried out within the linear range with respect to the quantity of the lipid using commercially purchased ganglioside GM1 (Sigma G7641, Sigma, MO, USA) as the standard.

Histopathological study

Paraffin sections (10 μm thick) were processed and used for hematoxylin/eosin staining. Frozen sections (15 μm thick) were reacted with X-gal by β-Gal staining Kit (Invitrogen Corp., Carlsbad, CA, USA) to visualize β-galactosidase activity. Ganglioside GM1 accumulated in the brain was visualized in frozen sections by immunostaining of avidin:biotinylated enzyme complex method with anti-GM1 ganglioside monoclonal antibody conjugated with biotin (Seikagaku Corp., Tokyo, Japan) and VECTASTAIN™ ABC Kit (Vector Laboratories, CA, USA). The staining procedures were carried out according to the instructions of the company.

The percentage of the infected cells was analyzed in the brain and the liver specimen stained with X-gal by measuring the blue-stained areas in the pictures.

Acknowledgements

We thank Dr Junichiro Matsuda at the National Institute of Infectious disease, Tokyo, for providing us β-galactosidase knockout mouse. We also thank Dr Kunihiko Suzuki in the University of North Carolina at Chapel Hill, and Dr Marie T Vanier in University of Lyon, France, for their critical readings of the manuscript and many helpful suggestions.

This work was supported by grants AT-11694306 and AT-11557060 from the Ministry of Education, Culture, Sports, Science, and Technology of Japan.

References

1 Birkenmeier EH *et al*. Increased life span and correction of metabolic defects in murine MPSVII after syngeneic bone marrow transplantation. *Blood* 1991; 78: 3081–3092.
2 Ohashi T *et al*. Adenovirus-mediated gene transfer and expression of human β-glucuronidase gene in the liver, spleen, and central nervous system in mucopolysaccharidosis type VII mice. *Proc Natl Acad Sci USA* 1997; 94: 1287–1292.
3 Konfeld S. Trafficking of lysosomal enzyme. *FASEB J* 1987; 1: 462–468.
4 Sands MS *et al*. Murine mucopolysaccharidosis type VII: long term therapeutic effects of enzyme replacement and enzyme replacement followed by bone marrow transplantation. *J Clin Invest* 1997; 99: 1596–1605.
5 Kakkis ED, Muenzer J, Tiller GE, Waber L. Enzyme replacement therapy in mucopolysacharidosis I. *N Engl J Med* 2001; 344: 182–188.
6 Hoogerbrugge PM *et al*. Allogenic bone marrow transplantation for lysosomal storage diseases. *Lancet* 1995; 345: 1398–1402.
7 Suzuki K *et al*. The Twitcher mouse: central nervous system pathology after bone marrow transplantation. *Lab Invest* 1998; 58: 302–309.
8 Matzner U *et al*. Long-term expression and transfer of arylsulfatase A into brain of arylsulfatase A-deficient mice transplanted with bone marrow expressing the arylsulfatase A cDNA from a retroviral vector. *Gene Therapy* 2000; 7: 1250–1257.
9 Pastores GM, Sibille AR, Grabowski GA. Enzyme therapy in Gaucher disease type I: dosage efficacy and adverse and effects in 33 patients treated for 6 to 24 months. *Blood* 1993; 82: 408–416.
10 Desnick RJ, Banikazemi M, Wasserstein M. Enzyme replacement therapy for Fabry disease, an inherited nephropathy. *Clin Nephrol* 2002; 57: 1–8.
11 Imaizumi M *et al*. Long term effects of bone marrow transplantation for inborn errors of metabolism: a study of four patients with lysosomal storage disease. *Acta Pediat Jpn* 1994; 36: 30–36.
12 Elliger SS *et al*. Elimination of lysosomal storage in brains of MPS VII mice treated by intrathecal administration of an adeno-associated virus vector. *Gene Therapy* 1999; 6: 1175–1178.
13 Frisella WA *et al*. Intracranial injection of recombinant adeno-associated virus improves cognitive function in a murine model of mucopolysaccharidosis type VII. *Mol Ther* 2001; 3: 351–358.
14 Shen JS, Watabe K, Ohashi T, Eto Y. Intraventricular administration of recombinant adenovirus to neonatal Twitcher mouse leads to clinicopatholgical improvements. *Gene Therapy* 2001; 8: 1081–1087.

15 Sands MS *et al*. Syngenic bone marrow transplantation reduces hearing loss associated with murine mucopolysaccharidosis type VII. *Blood* 1995; **86**: 2033–2040.
16 O'Connor LH *et al*. Enzyme replacement therapy for murine mucopolysaccharidosis type VII leads to improvements in behavior and auditory function. *J Clin Invest* 1998; **101**: 1394–1400.
17 Volger C *et al*. Enzyme replacement therapy in murine mucopolysaccharidosis type VII: neuronal and glial response to β-glucuronidase requires early inhibition of enzyme replacement therapy. *Ped Res* 1999; **45**: 838–844.
18 Day TM *et al*. Neonatal gene transfer leads to widespread correction of pathology in a murine model of lysosomal storage disease. *Proc Natl Acad Sci USA* 1999; **96**: 11288–11294.
19 Day TM *et al*. Prevention of systemic clinical disease in MPS VII mice following AAV-mediated neonatal gene transfer. *Gene Therapy* 2001; **8**: 1291–1298.
20 Suzuki Y, Oshima A, Nanba E. β-Galactosidase deficiency (β-galactosidosis): GM1 gangliosidosis and Morquio B disease. In: Scriver CR, Beaudet AL, Sly WS, Valle D (eds) *The Metabolic and Molecular Bases of Inherited Disease*, 8th edn. McGraw-Hill: New York, 2001, pp 3775–3803.
21 Stewart PA, Hayakawa EM. Interendothelial junctional change underlie the developmental 'tightening' of the blood–brain barrier. *Dev Brain Res* 1987; **32**: 271–281.
22 Matsuda J *et al*. Neurological manifestations of knockout mice with β-galactosidase deficiency. *Brain Dev* 1997; **19**: 19–20.
23 Matsuda J *et al*. β-Galactosidase-deficient mouse as an animal model for GM1-gangliosidosis. *Glycoconjugate J* 1997; **14**: 729–736.
24 He TC *et al*. A simplified system for generating recombinant adenoviruses. *Proc Natl Acad Sci USA* 1998; **95**: 2509–2514.
25 Nanba E, Suzuki K. Molecular cloning of mouse acid β-galactosidase cDNA : sequence, expression of catalytic activity and comparison with human enzyme. *Biochem Biophys Res Comm* 1990; **173**: 141–148.
26 Suzuki K. Enzymatic diagnosis of sphingolipidosis. *Methods Enzymol* 1987; **138**: 727–762.
27 Bradford MM. A rapid and sensitive method for the quantitation of microgram quantities of protein utilizing the principle of protein-dye binding. *Anal Biochem* 1976; **72**: 255–260.
28 Fujita N *et al*. Targeted disruption of the mouse sphingolipid activator protein gene: a complex phenotype, including severe leukodystrophy and wide-spread storage of multiple sphingolipids. *Hum Mol Genet* 1996; **5**: 711–725.
29 Hahn CN *et al*. Generalized CNS disease and massive GM1-ganglioside accumulation in mice defective in lysosomal acid β-galactosidase. *Hum Mol Genet* 1997; **6**: 205–211.
30 Svennerholm L. Estimation of sialic acids. II. A colorimetric resorcinol-hydrochloric acid method. *Biochem Biophys Acta* 1957; **24**: 604–611.

Available online at www.sciencedirect.com
SCIENCE DIRECT®
Biochemical and Biophysical Research Communications 312 (2003) 277–284
BBRC
www.elsevier.com/locate/ybbrc

Regulatory sequence elements of mouse GLUT4 gene expression in adipose tissues☆

Shinji Miura,[a] Nobuyo Tsunoda,[a] Shinobu Ikeda,[a] Yuko Kai,[a] Misaki Ono,[a] Kayo Maruyama,[a] Mayumi Takahashi,[a] Keiji Mochida,[b] Junichiro Matsuda,[c] M. Daniel Lane,[d] and Osamu Ezaki[a,*]

[a] *Division of Clinical Nutrition, National Institute of Health and Nutrition, 1-23-1 Toyama, Shinjuku-ku, Tokyo 162-8636, Japan*
[b] *Bioresource Center, The Institute of Physical and Chemical Research 3-1-1 Koyadai, Tsukuba-shi, Ibaraki 305-0074, Japan*
[c] *Department of Veterinary Science, National Institute of Infectious Diseases, 1-23-1 Toyama, Shinjuku-ku, Tokyo 162-8640, Japan*
[d] *Department of Biological Chemistry, Johns Hopkins University, 725 North Wolfe Street, Baltimore, MD 21205, USA*

Received 7 October 2003

Abstract

Ablation of GLUT4 in adipose tissues results in whole body insulin resistance and high-fat feeding down-regulates GLUT4 mRNA in white adipose tissues. Previous studies demonstrated that adipose tissue specific element(s) (ASE) of the murine GLUT4 gene is located between −551 and −442 relative to transcription start site and that high-fat responsive element(s) (HFRE) for down-regulation of the GLUT4 gene is located between bases −1001 and −442. To further characterize these regulatory elements, the regulation of GLUT4 minigenes containing −701, −551, and −506 bp of 5′-flanking region was studied in transgenic mice. GLUT4 minigene mRNA from −506 transgenic mice did not express in adipose tissues, indicating that ASE located within 45 bp is located between bases −551 and −506. An 80-kDa of nuclear DNA binding protein was found to bind to a -TCCTCGTGGGAAGCG- element located between bases −551 and −537. High-fat diet feeding down-regulated GLUT4 minigene mRNA in −701 transgenic mice, but not in −551 transgenic mice, indicating that HFRE is located within 150 bp between bases −701 and −551 of the GLUT4 gene and is distinct from ASE.

Keywords: Glucose transport; Fat intake; Adipose tissue; Insulin resistance; Transporter protein

Glucose transport into the cell is the rate-limiting step in insulin-activated glucose clearance under physiological conditions [1–3]. GLUT4, the insulin-responsive glucose transporter, is expressed in skeletal muscles, heart, and adipose tissues, and plays a major role for glucose transport [4]. Although skeletal muscle tissue accounts for the majority of whole body insulin-stimulated glucose uptake, adipose tissues also play an important role for maintenance of insulin sensitivity in vivo. Especially, the amount of GLUT4 is one of the critical factors in adipose tissues; the insulin resistance in skeletal muscles is a result of impaired signaling pathway from insulin receptor to GLUT4 vesicle [5], whereas a decrease of GLUT4 protein is a major cause of insulin resistance in adipose tissues [6]. Transgenic mice with overexpressed GLUT4 selectively in adipose tissues display increased insulin sensitivity [7]. Ablation of GLUT4 in adipose tissues caused insulin resistance in skeletal muscles by unknown mechanism(s) [8]. In the experimental high-fat diet-induced insulin resistance, the effect of the diet consumption to reduce GLUT4 gene expression preferentially affects adipocytes [9]. In addition, decreases in GLUT4 protein and mRNA levels in white adipose tissues (WAT) but not in skeletal muscles have been reported in NIDDM and obese patients

☆ *Abbreviations:* ASE, adipose tissue specific element(s); HFRE, high-fat responsive element(s); WAT, white adipose tissue; BAT, brown adipose tissue; C/EBP, CCAAT/enhancer-binding protein; PPAR, peroxisome proliferator-activated receptor; LXR, liver X receptor.

* Corresponding author. Fax: +81-3-3207-3520.
E-mail address: ezaki@nih.go.jp (O. Ezaki).

0006-291X/$ - see front matter © 2003 Elsevier Inc. All rights reserved.
doi:10.1016/j.bbrc.2003.10.114